Journal of Controlled Release 324 (2020) 104–123

Contents lists available at ScienceDirect

Journal of Controlled Release

journal homepage: www.elsevier.com/locate/jconrel

Near-infrared photocontrolled therapeutic release *via* upconversion nanocomposites

Zhimin Wang[a], Do Cong Thang[a], Qingyu Han[a], Xuan Zhao[b], Xilei Xie[c], Zhiyong Wang[d], Jun Lin[e], Bengang Xing[a,*]

[a] Division of Chemistry and Biological Chemistry, School of Physical & Mathematical Sciences, Nanyang Technological University, 637371, Singapore
[b] National and Local Joint Biomedical Engineering Research Center on Photodynamic Technologies, College of Chemistry, Fuzhou University, Fuzhou 350116, Fujian, China
[c] College of Chemistry, Chemical Engineering and Materials Science, Key Laboratory of Molecular and Nano Probes, Ministry of Education, Collaborative Innovation Center of Functionalized Probes for Chemical Imaging in Universities of Shandong, Shandong Normal University, Jinan 250014, China
[d] School of Materials Science and Engineering, Sun Yat-Sen University, Guangzhou 510275, China
[e] State Key Laboratory of Rare Earth Resource Utilization, Changchun Institute of Applied Chemistry, Chinese Academy of Sciences, Changchun 130022, China.

ARTICLE INFO

Keywords:
Near-infrared light
Photocontrolled release
Upconversion nanocomposites
Therapeutics
Bioimaging

ABSTRACT

Photocontrolled therapeutic release holds great promise due to its versatile manipulability, superb spatiotemporal precision and minimal tissue invasiveness in biomedical purposes. However, most of light-responsive platforms thus far have relied on UV or visible light which substantially limit the potential applicability in living animals. In recent decades, near-infrared (NIR) light-mediated theranostic upconversion nanocomposites (UCNCs) that integrate conventional UV/Vis-sensitive materials and classic lanthanide-doped upconversion nanoparticles (UCNPs) have significantly promoted the development of deep-tissue photoreleasable therapeutics *in vivo*. Herein, we seek to review current NIR upconversion triggered photorelease techniques and their diverse applications in the biological regulation, as well as diseases therapy. In addition, the future perspectives and challenges for advancing UCNCs based NIR photoreleasable nanotherapeutics into clinical translations are proposed.

1. Introduction

Currently, targeted therapy in clinical trials shows great promise against life threatening diseases, such as cancer, antibiotic-resistant infections and neurodegenerative disorders [1–5]. The development of drug delivery systems has opened doors to achieve more precise and effective diseases management, mainly owing to their unique therapeutic controllability over the dosage, location and timing [6,7]. In this regard, various smart stimuli-responsive platforms by either endogenous- (e.g. enzyme, pH, redox, hypoxia etc.) or external-factors (e.g., electricity, ultrasound, magnetic field, ionizing irradiation, light etc.) have been widely reported and utilized in site-specific targeting of therapeutic agents [8–11]. Despite the enormous progress, the practical applicability, efficacy and biosafety of these therapeutics rise increasing concerns for further clinical translations. For example, the endogenous stimuli-activated drug delivery systems face challenges of low specificity for the accumulation of therapeutic molecules in the disease tissues; while external stimuli-triggered therapeutic release is always limited by unsatisfied precision, unpleasant tissue invasiveness and potential complications [12,13].

Comparatively, the light-mediated drug-uncaging approaches have attracted considerable interest in the healthcare management, due to the fact that light can be tightly focused and manipulated in highly spatiotemporal accuracy [14–16]. The mechanisms of most photo-triggered drug delivery systems are based on ultraviolet (UV) light-induced chemical structures breaking or conformational switch, which raise the concerns of potential phototoxicity and unsatisfied penetrability in living conditions [17]. Gratifyingly, recent advances in near-infrared (NIR, 650 - 1000 nm) light-controlled theranostic release have greatly overcome the disadvantage of UV light, enabling the possibility of noninvasive, biocompatible and precise diseases therapy in deep tissues [14,18–20]. Among the methodologies of NIR photo-controlled drug delivery, the utilization of biophotonic nanomaterials, especially upconversion nanoparticles (UCNPs) as versatile NIR-to-UV/vis optical transducers to generate in situ high intensity light source, achieving on-demand therapeutics photorelease with less adverse effects and better tissue penetration [21,22].

Despite the superb photonic feature of anti-stokes shift upconversion luminescence (UCL), it should be noted that UCNPs for practical therapeutic purposes usually require further functionalization to be

* Corresponding author.
E-mail address: Bengang@ntu.edu.sg (B. Xing).

https://doi.org/10.1016/j.jconrel.2020.05.011
Received 20 March 2020; Received in revised form 30 April 2020; Accepted 5 May 2020
Available online 11 May 2020
0168-3659/

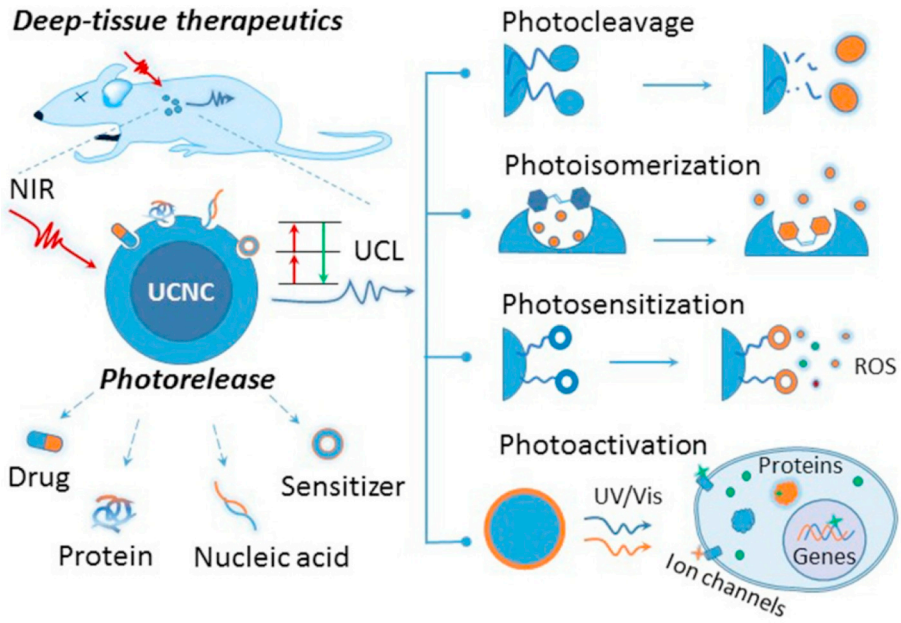

Scheme 1. Upconversion nanocomposites for NIR photocontrolled therapeutic release.

biocompatible nanocarriers for drugs or bioactive molecules loading. To achieve photo-responsive deliver capabilities, various upconversion nanocomposites (UCNCs) through combining conventional UV-Vis-sensitive chemical structures or supramolecular polymeric biomaterials have been reported in the past decade [23–25]. These multifunctional UCNCs enable simultaneous diseases (or bioindicators) sensing and NIR photocontrolled therapeutics release. Additionally, recent studies have demonstrated that UCNPs display promising photon-downconversion properties, which allowed bioimaging and theranostic applications in the second NIR window (NIR-II) with enhanced tissue penetration depth and quantum efficacy [26–30].

Hence in this work, we will systematically review recent theranostic UCNCs facilitated NIR photorelease techniques (Scheme 1), including photocleavage, photoisomerization, photosensitization and photoactivation. In addition, their diverse biomedical applications in remote-controlled diseases therapy as well as biofunctional regulations are summarized in detail. Finally, to promote UCNCs-based NIR photo-responsive nanotherapeutics for clinical translations, future challenges and perspectives are discussed as well.

2. Photon upconversion of upconversion nanocomposites (UCNCs)

So far, there have been comprehensive introduction about the preparation, functionalization and theranostic applications of rare-earth ions-doped UCNPs [31–34]. Generally, UCNPs structures compromise three essential components including host matrix (e.g. Y^{3+}, Gd^{3+}), sensitizer (e.g. Yb^{3+}) and emitters (dopant lanthanide ions). In which, the host materials play important roles in the upconversion luminescence (UCL) processes. The typical excitation wavelength of Yb^{3+}-based UCNPs is 980 nm, and it is likely to be shifted to ~ 800 nm by doping Nd^{3+} sensitizer as the energy transfer bridge (Scheme 2a-b) [35]. In addition, the multicolor UCL from the UV-Vis to NIR range can be manipulated through controlling the combination and concentration of lanthanide dopants (Scheme 2c).

Despite the optical multiplicity of UCNPs, the relatively low upconversion quantum yields (Φ) are considerable challenges for practical photo-regulation utilizations. The past decade witnessed the great efforts to improve the photon upconversion efficiency, innovative strategies through rational energy-transfer manipulation, crystal-lattice modification, fabrication of core-shell structures, as well as ingenious integration of UCNPs with other plasmonic nanomaterials or organic dyes have been developed [37–39]. These UCL-enhanced nanoplatforms further contribute to the biophotonic applications, in bioimaging, biosensing and therapeutics.

In light with the superior feature of NIR to UV/Vis photon upconversion, UCNPs can act as promising deep-tissue phototheranostics with a wide range of applications, such as precise photo-triggered drug delivery, photodynamic/photothermal therapy and optogenetic regulation. UCNPs as the luminescent contrast agents can be directly used for bioimaging, however, it is needed further functionalization to improve the biocompatibility and introducing therapeutic roles. Accordingly, a variety of upconversion nanocomposites (UCNCs) through combination of UCNPs and bioactive materials are developed for biomedical studies in recent years [23,24,40,41].

As shown in Scheme 3, the design of phototheranostic UCNCs also covers three main components, (i) UCNP-based nanocore, which is used as both optical transducers and nanocarriers; (ii) surface coatings, compromising silicon or various polymers (e.g. polyethylenimine (PEI), polyacrylic acid (PAA) and polyethylene glycol (PEG) etc.) that play the role in improving the biocompatibility, and enabling biomolecules encapsulation, tissue-targeting/accumulation as well as light-senstitive release; (iii) therapeutic agents, including clinical drugs, peptides, antibodies, nucleic acids (DNA or RNA) and photosensitizers, these molecules can be precisely released or activated *via* UCL-triggered upconversion photochemistry under NIR laser irradiation.

3. NIR photocontrolled release techniques and therapeutic applications

So far, UV/Vis light-mediated photochemistry and its applications in photocontrolled drug delivery have been introduced extensively [15,17,42]. There are also some recent works reviewed the fundamentals and typical utilizations of UCNPs-assisted photochemistry for NIR phototherapy [43,44]. With the aim to provide a systematic review, in this section we will specifically focus on UCNCs-based photorelease techniques such as photocleavage, photoisomerization, photosensitization and photoactivation, meanwhile the design strategies, response mechanisms and properties are described. In addition, the technical characteristics (e.g. formulation, coating, excitation/emission wavelength of UCNPs, NIR laser power density and typical photo-

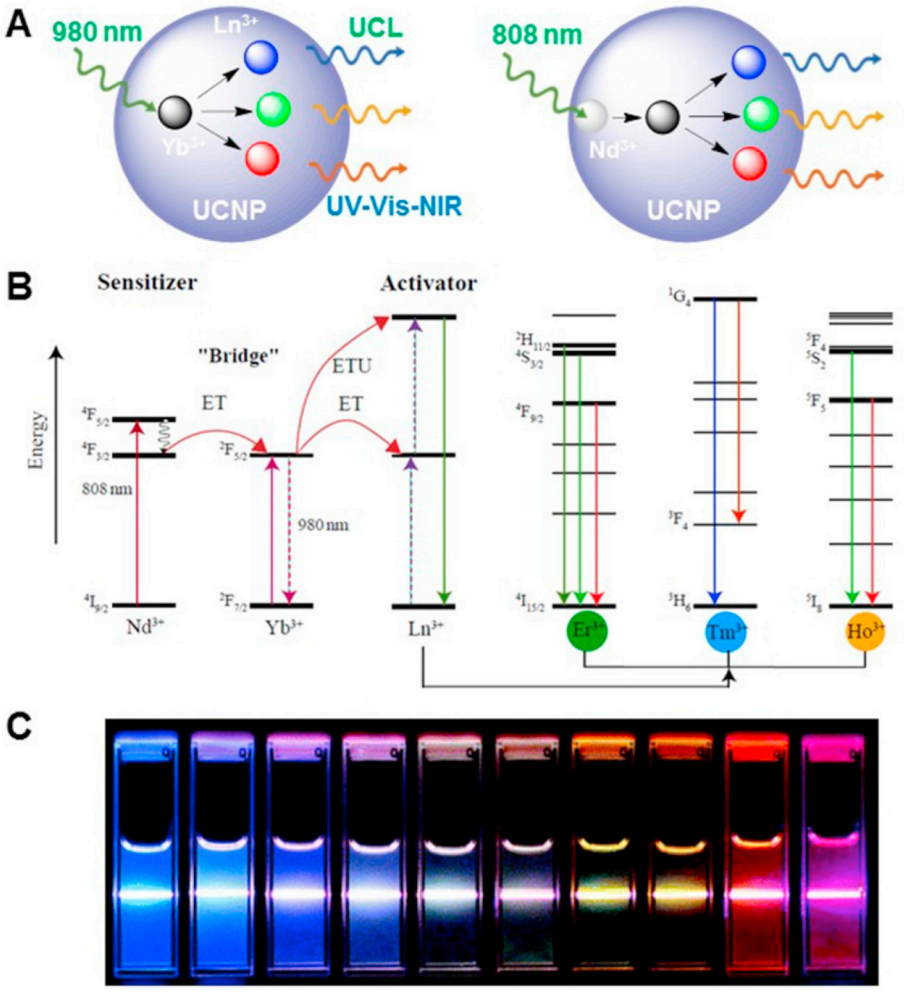

Scheme 2. Typical design the properties of upconversion nanoparticles (UCNPs). (A) 980 nm- and 808 nm-excited UCNPs. (B) Proposed energy transfer mechanisms of the upconversion process. (C) Upconversion luminescence (UCL) photographs. UCL photograph was reproduced with permission [36]. Copyright 2008, American Chemical Society.

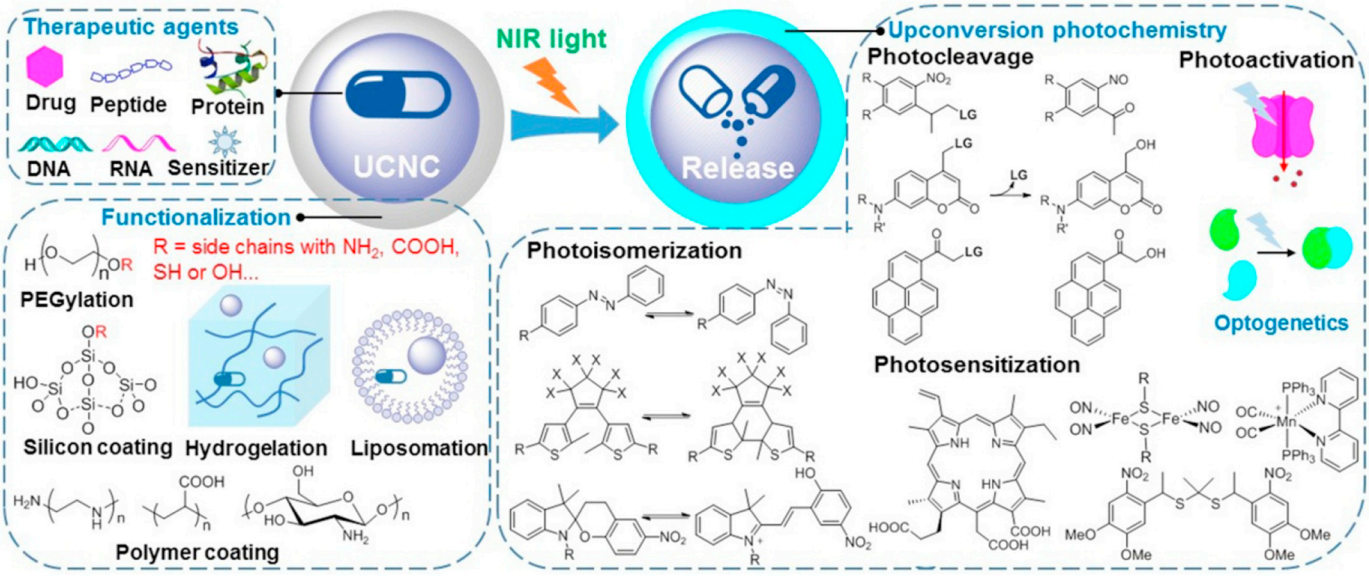

Scheme 3. Preparation, functionalization and NIR upconversion photochemistry for photocontrolled therapeutics release with UCNCs.

Table 1
Brief summary of UCNCs-based NIR photorelease techniques and theranostic applications.

Principles	Photosensitive moieties	UCNCs	Ex. / UCL[a]	Power density[b]	Applications	Ref
Photocleavage	3, 5-dialkoxy-benzoin	$NaYF_4$:Yb/Tm@3,5-di(carboxymethox y) benzoin acetate	980 nm / 290 nm	550 W/cm^2	Photorelease of small molecules in solution	[45]
	O-nitrobenzyl derivatives	$NaYF_4$:Yb/Tm@$NaYF_4$@PEO-b-PNBMA	980 nm / 360 nm	5 W (Power)	Photorelease through UCL-triggered block copolymer micelles dissociation	[46]
		$NaYF_4$:Yb/Tm@$NaYF_4$@Polyacrylamide-PEG		5 W (Power)	Photorelease of enzyme through UCL-triggered hydrogel degradation	[47]
		$LiYF_4$:Yb/Tm@SiO_2@GPS@CH/PhL		1.8 W/cm^2	Photorelease of enzyme through UCL-triggered hydrogel degradation *in vitro*	[48]
		$NaYF_4$:Yb/Tm@Polymer		1 W (Power)	Photorelease of small molecules through UCL-triggered polymer degradation	[49,50]
		$NaYF_4$:Yb/Tm@$NaYF_4$@SiO_2-D-luciferin		255 W/cm^2	Photorelease of D-luciferin for *in vitro* and *in vivo* bioimaging	[51]
		$NaYF_4$:Yb/Tm@$NaYF_4$@SiO_2		-	Photorelease of drug doxorubicin	[52]
		$NaYF_4$:Yb/Tm@$NaYF_4$@SiO_2/PAMAM		1 W (Power)		[53]
		$NaYF_4$:Yb/Tm@SiO_2-DNA/siRNA		2.8 - 5.6 W/cm^2	Photorelease of DNA/siRNA *in vitro* and *in vivo*	[54]
		$NaYF_4$:Yb/Tm@$NaYF_4$@SiO_2-siRNA		-	Photorelease of siRNA *in vitro*	[55]
		$NaYF_4$:Yb/Tm@$NaYF_4$@SiO_2-FA/DOX		1.8 W/cm^2	Photorelease of doxorubicin *in vitro* and *in vivo*	[56]
		$NaYF_4$:Yb/Tm@ SiO_2-PKA		5 W/cm^2	Photoactivation of PKA *in vitro*	[57]
		$NaYF_4$:Yb/Tm@$NaYF_4$@ONB-FU		63.2 mW/cm^2	Photorelease of drug 5-fluorouracil	[58]
		$NaYF_4$:Yb/Tm/CaF_2@PEI/Fluorescein	975 nm / 360 nm	2.6 W/cm^2	Photouncaging of fluorescein	[59]
	Coumarin derivatives	$NaYF_4$:Yb/Tm@$NaLuF_4$@SiO2@Chlorambucil	980 nm / 360 nm	50 mW/cm^2	Photorelease of drug chlorambucil	[60]
	Platinum(IV) complex	$NaYF_4$:Yb/Tm@$NaYF_4$@SiO2@platinum(IV) complex	980 nm / 360 nm	-	Photorelease of drug platinum(II) complex *in vitro* and bioimaging	[61]
		$NaYF_4$:Yb/Tm@$NaGdF_4$:Yb@PEI/DPP/PEG-platinum(IV) complex		2.5 W/cm^2	Photorelease of drug platinum(II) complex and multimodal bioimaging both *in vitro* and *in vivo*	[62]
		$NaYF_4$:Yb/Er@Polymer-platinum(IV) complex/ RhB	980 nm / 550 nm	-	Photorelease of drug platinum(II) complex and bioimaging both *in vitro* and *in vivo*	[63]
		$NaYF_4$:Yb/Tm@$NaYF_4$@DSPE-PEG/platinum (IV) complex	980 nm / 360 nm	7.3 W/cm^2	Photorelease of drug platinum(II) complex in solution	[64]
		$NaGdF_4$:Yb/Tm (or Er)@SiO_2-platinum(IV) complex	980 nm / 360 nm (or 550 nm)	0.12 W (Power)	Photorelease of drug platinum(II) complex *in vitro*	[65]
		$NaYF_4$:Yb/Tm@$NaGdF_4$:Yb@$NaNdF_4$:Yb@ SiO_2-DOX/platinum(IV) complex	808 nm / 360 nm	3 W/cm^2	Photorelease of drugs chlorambucil and platinum(II) complex *in vitro* and *in vivo*	[66]
		$NaYF_4$:Yb/Tm@PEI-platinum(IV) complex	980 nm / 360 nm	0.72 W/cm^2	Photorelease of drug platinum(II) complex *in vitro* and *in vivo*	[67]
	Ruthenium complex	$NaYF_4$:Yb/Tm@$NaYF_4$@$mSiO_2$	974 nm / 480 nm	0.35 W/cm^2	Photorelease of doxorubicin *in vitro*	[68]
		NaGdF4:Yb/Tm/Ca@NaYbF4:Ca@ NaNdF4:Gd/Ca@$mSiO_2$/DOX/Ru complex	808 nm / 480 nm	0.75 W/cm^2	Photorelease of doxorubicin *in vitro* and *in vivo*	[69]
	$^1O_2$-sensitive linkers	$NaYF_4$:Yb/Er@$mSiO_2$ − MB/ $mSiO_2$-β-CD	980 nm / 550, 660 nm	2 W/cm^2	Photorelease of small molecules *in vitro* and bioimaging	[70]
	Pyrenemethyl ester derivatives	$NaYF_4$:Yb/Tm@$NaLuF_4$ @$mSiO_2$-Py/β-CD	980 nm / 360 nm	1.5 W/cm^2	Photorelease of drug *in vitro* and bioimaging	[71]
	Roussin's black salt (RBS)	$NaYF_4$:Yb/Tm@$NaYF_4$@$mSiO_2$/PAH	980 nm / 550, 660 nm	4.5 W (Power)	Photorelease of NO and tumor therapy *in vitro*	[72]
		PDMS@$NaYF_4$:Gd/Yb/Tm(Er)	980 nm / 480, 550, 660 nm	28 W/cm^2		[73]
		$NaYbF_4$:Tm@$NaYF_4$:Yb/Er		1 W/cm^2		[74]
		$NaYbF_4$:Tm@$NaYF_4$:Yb/Nd@$NaYF_4$	808 nm / 360 nm	0.75 W/cm^2	Synergistic NO and DOX delivery for antitumor therapy *in vitro* and *in vivo*	[75]
	$Mn(bpy)(PPh_3)_2(CO)_2$	$NaYF_4$:Yb/Tm	980 nm / 480 nm	2 W (Power)	Photorelease of CO	[76]
	$[Fe(\eta_5\text{-Cp})(CO)_2I]$	$NaGdF_4$:Yb/Er@SiO_2	980 nm / 550, 660 nm	1 W/cm^2		[77]
	PS[c]	$LiYF_4$:Yb/Tm@PEG/ODA	980 nm / 365, 480 nm	20 W/cm^2	Photorelease of H_2S	[78]
Photoisomerization	Dithienylethene	$NaYF_4$:Yb/Tm@Polymer	980 nm / 360 nm	556 W/cm^2	Photorelease of molecules in solution	[79]
	Azobenzen	$NaYF_4$:Yb/Tm@$NaYF_4$@$mSiO_2$/DOX		2.4 W/cm^2	Photorelease of doxorubicin *in vitro*	[80]
		$NaGdF_4$:Yb/Tm@$NaGdF_4$@Azo-Lipo/DOX		2.2 W/cm^2	Photorelease of doxorubicin *in vitro* and *in vivo*	[81]
		$NaYF_4$:Yb/Tm/Er@PEG-α-CD/siRNA		0.75 W/cm^2	Photorelease of siRNA *in vitro*	[82]
	Spiropyran	$NaYF_4$:Yb/Tm@Polymer/ Coumarin 102		4.7 W/cm^2	Photorelease of small molecules *in vitro*	[83]
		$NaYF_4$:Yb/Er/DNA	980 nm / 550, 660 nm	0.5 W/cm^2	Photorelease of proteins *in vitro*	[84]

(*continued on next page*)

Table 1 (*continued*)

Principles	Photosensitive moieties	UCNCs	Ex. / UCL[a]	Power density[b]	Applications	Ref
Photoactivation	LOV2-STIM1/ORAI1	$NaYF_4$:Yb/Tm@$NaYF_4$@PAA/Antibody	980 nm / 480 nm	15 - 50 mW/mm^2	Optogenetic activation Ca^{2+} signaling for immunomodulation *in vitro* and *in vivo*	[85]
	ChR2	$NaYF_4$:Yb/Tm@$NaYF_4$@PLGA		1 W (Power)	Optogenetic activation of Ca^{2+} channel *in vitro*	[86]
		$NaYF_4$:Yb/Tm@SiO_2		4 W (Power)	Optogenetic activation of Ca^{2+} channel *in vitro* and in *C. elegans*	[87]
		$NaYbF_4$:Tm@$NaYF_4$		5 W/cm^2	Optogenetic activation of ChR2 *in vitro*	[88]
		$NaYF_4$:Yb/Tm@SiO_2/PEG		22.6 mW/mm^2		[89]
		$NaYF_4$:Yb/Tm		20 mW/mm^2	Optogenetic stimulation of the spinal cord in behaving animals	[90]
		$NaYF_4$:Yb/Tm/Nd@ $NaYF_4$@PAA	808 nm / 480 nm	0.8 W/cm^2	Optogenetic activation of Ca^{2+} channel *in vitro* and in zebrafish	[91]
	C1V1, mChR1, PsChR	$NaYF_4$:Yb/Sc/Er or $NaYF_4$:Yb/Sc/Tm@$NaYF_4$	980 nm / 550 or 480 nm	41 mW/mm^2	Optogenetic activation of various ChRs *in vitro*	[92]
	ChR2, C1V1	$NaYF_4$:Yb/Tm@$NaYF_4$ $NaYF_4$:Yb/Er@$NaYF_4$	980 nm / 480 or 550 nm	7 or 4 mW/mm^2	Multiplexed optogenetic activation or inhibition of neurons *in vitro* and *in vivo*	[93,94]
	ReaChR	$NaYF_4$:Yb/Er@$NaYF_4$@ Dye@F127	800 nm / 550 nm	2 W/cm^2	Optogenetic activation of hippocampal neurons *in vitro*	[95]
	eNpHR	$NaYF_4$@$NaYF_4$:Yb/Er@ $NaYF_4$	980 nm / 550 nm	6 mW/mm^2	Optogenetic inhibition of neurons *in vitro* and *in vivo*	[96]
	ChR2, Arch	$NaYF_4$:Yb/Tm@SiO_2 $NaYF_4$:Yb/Er@SiO_2	980 nm / 480 or 550 nm	1.4 W/mm^2	Optogenetic deep brain activation and inhibition	[97]
	Chrimson	$NaGdF_4$:Yb/Er/Ca @ $NaYbF_4$:Gd/Ca@ $NaNdF_4$:Gd/Ca@DSPE-PEG	808 nm / 550 nm	0.64 W/mm^2	Optogenetic manipulation of the *caenorhabditis elegans* motor circuit	[98]
	Jaw, VChR1	$NaErF_4$:Yb/Tm@ $NaYF_4$:Yb@ $NaNdF_4$:Yb	980 nm/660 nm 808 nm/550 nm	4 W (Power)	Programmable photoactivation of ion channels *in vitro*	[99]
	Cry2-FADD/Cib-Fas	$NaYF_4$:Yb/Tm@$NaGdF_4$:Yb	980 nm / 480 nm		Optogenetic activation of apoptosis signaling for cancer therapy	[100]
Photosensitization	Phthalocyanine (ZnPc or SiPc)	$NaYF_4$:Yb/Er@mSiO_2	980 nm / 540 and 660 nm	0.5 W (Power)	Photodynamic tumor therapy *in vitro* and/or *in vivo*	[101]
		$NaYF_4$:Yb/Er		2.5 W/cm^2		[102]
		$NaYF_4$:Yb/Er@PAAm		0.39 W/cm^2		[103]
		$NaGdF_4$:Yb/Ce/Ho@$NaGdF_4$		0.72 W/cm^2		[104]
		$NaYF_4$:Yb/Er@PEG		1 W/cm^2	Photodynamic and chemo-anticancer therapy *in vitro*	[105]
		$NaYF_4$:Yb/Er/Gd@ SiO_2		1.4 W/cm^2	Synergistic photodynamic and chemo-therapy *in vitro* and *in vivo*	[106]
		$NaGdF_4$:Yb/Ce/Ho@$NaGdF_4$@mSiO_2@ polymer	980 nm / 650 nm	0.72 W/cm^2	Synergistic DOX delivery and photodynamic therapy *in vitro* and *in vivo*	[107]
		$NaErF_4$:Yb/Tm@$NaYF_4$:Yb@$NaYF_4$:Yb/Nd@ SiO_2	980 nm/660 nm and 808 nm/540 nm	0.6 W/cm^2	Synergistic photodynamic and gene therapy *in vitro* and *in vivo*	[108]
				0.608 W/cm^2	Photodynamic tumor therapy and bioimaging *in vitro* and *in vivo*	[109]
	Chlorin e6 (Ce6)	$NaYF_4$:Yb/Er@$NaGdF_4$@DSPE-PEG	980 nm / 540 and 660 nm	0.6 W/cm^2		[110]
		NaY(Mn)F_4:Yb/Er@PAA/PAH		0.5 W/cm^2		[111]
		$NaGdF_4$:Yb/Er@PAA/PEI		0.8 W/cm^2	Synergistic siRNA delivery and photodynamic therapy *in vitro* and *in vivo*	[112]
		$NaYF_4$:Yb,Er@C18PMH-PEG		0.5 W/cm^2	Synergistic DOX delivery and photodynamic therapy *in vitro*	[113]
		$NaYF_4$:Yb,Er@$NaYF_4$@mSiO_2		1.5 W/cm^2		[114]
		$NaYF_4$:Yb/Er@PEG		0.5 W/cm^2	Photodynamic tumor therapy and immunotherapy *in vitro* and *in vivo*	[115]
		$NaYF_4$:Yb/Er/Nd@$NaYF_4$:Nd@PAA/PEG/ Peptide	808 nm / 540 and 660 nm	0.4 W/cm^2	Photodynamic tumor therapy and bioimaging *in vitro* and *in vivo*	[116]
		$NaYF_4$:Yb/Er/Nd@$NaYF_4$:Nd@MnO_2		0.5 W/cm^2	Photodynamic tumor therapy *in vitro* and *in vivo*	[117]
	Porphyrin	$NaGdF_4$:Yb/Er@$NaGdF_4$@PEG	980 nm / 480 nm	0.7 W/cm^2	Photodynamic tumor therapy and bioimaging *in vitro* and *in vivo*	[118]
		$NaYF_4$:Yb/Er@PEG/DNA (MOF)	980 nm / 540 and 660 nm	15.9 W/ cm^2	Photodynamic therapy *in vitro*	[119]
		$NaGdF_4$:Yb/Er@$NaGdF_4$@PVP (MOF)		1.2 W/cm^2	Photodynamic tumor therapy *in vitro* and *in vivo*	[120]
		$NaGdF_4$:Yb/Er@$NaGdF_4$:Yb/Nd@$NaGdF_4$@ PVP (MOF)	808 nm / 540 and 660 nm	1 W/cm^2		[121]
	Rose Bengal (RB)	$NaYF_4$:Yb/Er@AEP/PEG	980 nm / 540 and 660 nm	1.5 W/cm^2	Photodynamic tumor therapy and bioimaging *in vitro*	[122]

(*continued on next page*)

Table 1 (*continued*)

Principles	Photosensitive moieties	UCNCs	Ex. / UCL[a]	Power density[b]	Applications	Ref
		$NaYF_4$:Yb/Er@Dextran/PEG		1 W/cm^2	Photodynamic therapy *in vitro*	[123]
		$NaGdF_4$:Yb/Er@$NaGdF_4$:Yb/Nd@PEI	808 nm / 540 and 660 nm	0.52 W/cm^2	Photodynamic tumor therapy and bioimaging *in vitro* and *in vivo*	[124]
		$NaYF_4$:Yb/Ho@$NaYF_4$:Nd@$NaYF_4$@PAAm		1.62 W/cm^2	Photodynamic therapy *in vitro*	[125]
		$NaGdF_4$:Yb/Nd@$NaGdF_4$:Yb/Er@$NaGdF_4$@PAA/PEG		6 W /cm^2	Synergistic Pt(IV) activation and photodynamic therapy *in vitro*	[126]
		$NaYF_4$:Yb/Er@$NaYF_4$:Yb /Nd@$NaYF_4$@$mSiO_2$/PEG	795 nm / 540 and 660 nm	4 W /cm^2	Photodynamic therapy *in vitro*	[127]
		$NaYF_4$:Yb/Er/Tm@AEP/PEG	980 nm / 360, 480, 540, 660 nm	0.5 W /cm^2	Synergistic drug delivery, photodynamic therapy and bioimaging *in vitro* and *in vivo*	[128]
		$NaGdF_4$:Yb/Er@BSA	980 nm / 540 and 660 nm	13 W /cm^2	Photodynamic therapy *in vitro*	[129]
		$NaYF_4$:Yb/Er@SiO_2		0.6 W /cm^2	Suppression of Alzheimer's β-amyloid aggregation *in vitro*	[130]
	TiO_2	$NaYF_4$:Yb/Tm@$NaGdF_4$:Yb	980 nm / 360 nm	4.7 W /cm^2	Photodynamic tumor therapy *in vitro* and *in vivo*	[131]
		$NaYF_4$:Yb/Tm@SiO_2		1000 J/cm^2		[132,133]
		$NaGdF_4$:Yb/Tm@SiO_2		1.32 W (Power)	Synergistic photorelease of DOX and photodynamic therapy *in vitro*	[134]
		$NaYF_4$:Yb/Er@$NaYF_4$:Yb/Nd@PVP		4.7 W /cm^2	Photodynamic tumor therapy and multimodal bioimaging *in vitro* and *in vivo*	[135]
		$NaGdF_4$:Yb/Tm@$NaGdF_4$:Yb@$NaNdF_4$:Yb@$NaGdF_4$@$mSiO_2$	808 nm / 360 and 480 nm	-	Photodynamic tumor therapy and bioimaging *in vitro* and *in vivo*	[136]
	TiO_2 and hypocrellin A	$NaYF_4$:Yb/Tm@$NaYF_4$:Yb@$NaNdF_4$:Yb@$NaYF_4$@PVP/SiO_2/HA		2 W/cm^2		[137]
	CeO_2	mSiO2@Yb/Tm/Ce@PEG	980 nm / 360 and 480 nm	-	O_2-evolving synergetic, DOX release and photodynamic	[30]
		$NaGdF_4$:Yb/Tm@$mSiO_2$		0.72 W/cm^2	cancer therapy *in vitro* and *in vivo*	[138]
		$NaGdF_4$:Yb/Tm@$NaGdF_4$:Yb/Nd@gC_3N_4	808 nm / 360 and 480 nm	0.5 W/cm^2	Tri-mode imaging-guided photodynamic therapy	[139]
	Conjugated polyelectrolyte (CPE)	$NaYF_4$:Yb/Tm@CCPEB	980 nm / 360 nm	1.5 W/cm^2	Synergistic photorelease of DOX and photodynamic therapy *in vitro*	[140]
				2.6 W/cm^2	Synergistic photorelease of siRNA and photodynamic therapy *in vitro* and *in vivo*	[141]
	Re(I) complex	$NaYF_4$:Yb/Tm@$NaYF_4$@ PAA-chitosan		1.5 W/cm^2	Photodynamic anticancer therapy *in vitro*	[142]
	Riboflavin	$NaYF_4$:Yb/Tm@$NaYF_4$@TMAH	975 nm / 450 nm	1.5 W/cm^2	Photodynamic tumor therapy *in vitro* and *in vivo*	[143]
	Merocyanine 540 (MC540),	$NaYF_4$:Yb/Er@$mSiO_2$	975 nm / 540 and 660 nm	0.5 W/cm^2	Photodynamic tumor therapy and immunotherapy *in vitro* and *in vivo*	[144]
	KillerRed	$NaYF_4$:Yb/Er@$NaYF_4$@PAA		0.5 W/cm^2	Photodynamic tumor therapy *in vitro*	[145]

[a] It only indicates the major upconversion emission involved in specific photoreactions.
[b] NIR laser power density used in practice, especially for *in vivo* stimulation.
[c] PS indicates propane-2, 2-diylbis((1-(4,5-dimethoxy-2-nitrophenyl)ethyl)sulfane.

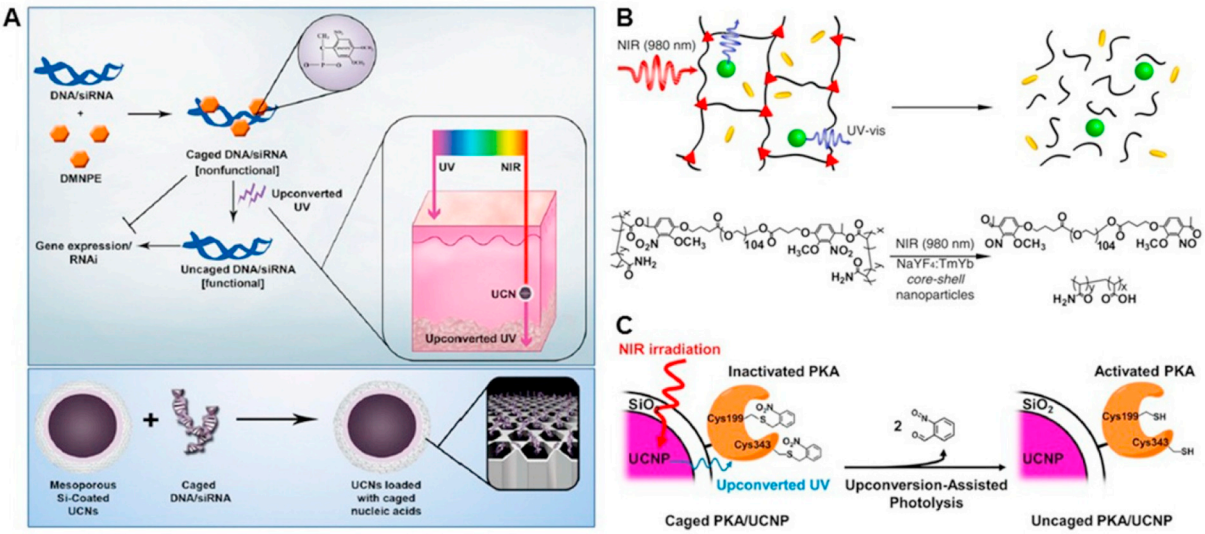

Fig. 1. Representative UCNCs for upconversion photocleavage-triggered biomolecules release. (A) NIR upconversion triggered photo-uncaging of plasmid DNA/siRNA. Reprinted with permission [54]. Copyright 2012, National Academy of Sciences. (B) NIR-light-triggered degradation of a photosensitive hydrogel for biomacromolecules release. Reprinted with permission [47]. Copyright 2012, American Chemical Society. (C) NIR upconversion-assisted photolysis for PKA activation. Reprinted with permission [57]. Copyright 2015, American Chemical Society.

responsive moieties) and theranostic applications (e.g. biomolecules regulation, neuronal modulation, antibacterial and antitumor therapy) have also been summarized in detail.

3.1. Upconversion photocleavage for biomolecules release and drug delivery

One typical approach used in upconversion photorelease is photocleavage, in which molecular payloads are covalently caged or conjugated on the surface of functionalized UCNPs. Briefly, there are three main design strategies: (1) NIR light illumination towards photoresponsive linkers (e.g. O-nitrobenzyl derivatives, coumarins etc.) that can directly uncage linked biomolecules, such as nucleic acids, proteins and drugs; (2) photocleavage induced degradation of the carrier layer on UCNPs that can enable release of loaded molecules; (3) photocleavage of bioactive donor molecules (e.g. gaseous donors). Relevant advances employing upconversion photocleavage for various theranostic release have been comprehensively summarized in Table 1 (the part of photocleavage), and some representative applications will be further synoptically reviewed below.

3.1.1. Biomolecules release

NIR photocontrolled release of biomolecules like nucleic acids and

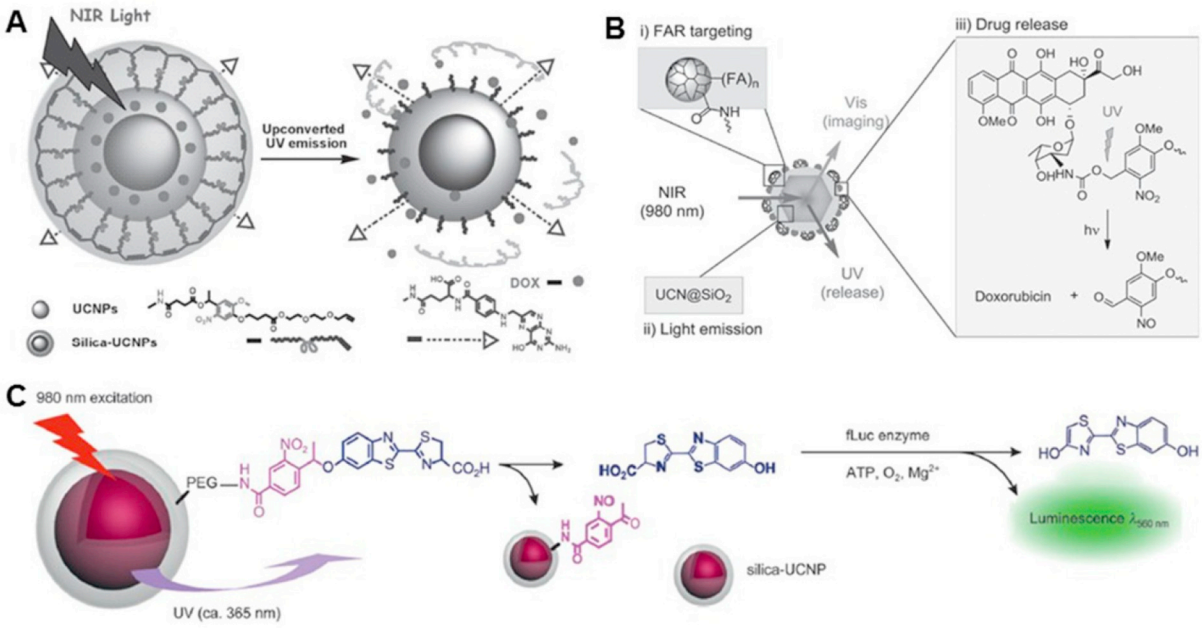

Fig. 2. Representative UCNCs for upconversion photocleavage-mediated anticancer drugs delivery. (A) NIR photocontrolled doxorubicin delivery through photocaged mesoporous silica coated UCNPs. Reprinted with permission [52]. Copyright 2013, Wiley-VCH. (B) NIR-excited upconversion nanocrystal (UCN) covalently linked with multivalent folate (FA)-conjugated dendrimer for folate receptor (FAR)-targeted cell imaging and light triggered release of DOX. Reprinted with permission [53]. Copyright 2015, Wiley-VCH. (C) Upconversion photo-uncaging mediated D-luciferin release and subsequent bioluminescence imaging. Reprinted with permission [51]. Copyright 2012, Wiley-VCH.

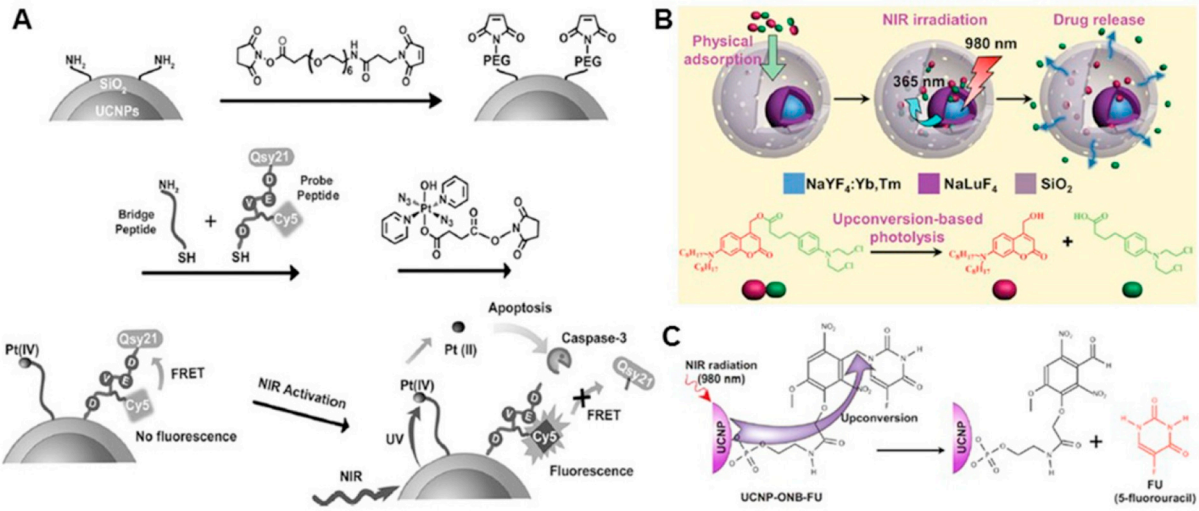

Fig. 3. Representative UCNCs for upconversion photocleavage-triggered prodrugs activation. (A) NIR light activation of anticancer platinum (IV) prodrug and intracellular apoptosis imaging. Reprinted with permission [61]. Copyright 2013, Wiley-VCH. (B) NIR upconversion-based photolysis of the prodrug chlorambucil. Reprinted with permission [60]. Copyright 2014, Wiley-VCH. (C) NIR light activation of 5-fluorouracil prodrug. Reprinted with permission [58]. Copyright 2014, American Chemical Society.

proteins has shown great promise in various biomedical applications. In particular, upconversion-based nucleic acids photorelease was widely applied in the research of gene therapy. To achieve effective gene delivery, UCNPs can be generally modified with positively charged materials, which enables both good gene-loading efficacy through electrostatic attractions and increased binding efficacy to the anionic plasma membranes [146]. Zhang et al. reported that photocaged nucleic acids could also be loaded into mesoporous silica ($mSiO_2$)-coated UCNCs (Fig. 1A), and this method significantly increased the loading efficiency of DNA/siRNA when compared to the chemical crosslinking strategy [54]. Furthermore, this technique enabled photocontrolled and specific GFP-gene expression/knockdown *in vitro* and *in vivo*. Besides, Xing et al. developed different upconversion nanoplatforms that siRNA was covalently and stably linked on the UCNCs surface by cationic photocaged linkers [55]. After cellular internalization and followed by 980 nm laser exposure, the UV emission effectively triggered siRNA release that was further confirmed by gene silencing tests. Fan et al. introduced charge-variable cationic conjugated polyelectrolyte brushes (CCPEB) functionalized UCNCs for NIR photocontrolled siRNA release [141]. Upon 980 nm irradiation, the positive-charged CCPE polymer with o-nitrobenzyl ester protection can be converted to zwitterionic conjugated polyelectrolyte brushes (ZCPEB) thereby inducing siRNA release *via* charge repulsion.

In addition to DNA/RNA delivery, several upconversion nanosystems have been employed for other macromolecules delivery. For example, Zhao et al. developed photosensitive hybrid hydrogel that UCNPs and proteins/enzymes were inactively entrapped, thus “on demand” photorelease of these proteins can be realized *via* UCL triggered gel−sol transition (Fig. 1B) [47]. In contrast to the carrier destruction approach, Lee et al. reported a NIR photoactivatable enzyme platform by immobilizing caged protein kinase A (PKA) on UCNPs surface (Fig. 1C) [57]. The NIR stimulation allowed selectively activate PKA and induced downstream cellular response in living cells with high spatiotemporal resolution.

3.1.2. Drug delivery

Engineering UCNCs as molecular nanocarriers for NIR light-responsive drug delivery has attracted tremendous attention in the field of precise tumor therapy. In 2013, Xing et al. encapsulated antitumor drug doxorubicin (DOX) within the UCNPs mesoporous silica layer capped by cross-linked photosensitive molecules (Fig. 2A) [52]. This photocontrolled drug delivery system demonstrated good efficiency for the real-time imaging and selective intracellular drug release with less photo-damage. Choi et al. designed another type of UCNCs that were modified through covalent attachment of photocaged DOX molecule (Fig. 2B) [53]. Such a nanoplatform enabled selective tumor targeting and effective NIR photo-uncaging of DOX. Besides, Yeh et al. further introduced the formulation and application of UCNCs as NIR-triggered drug delivery vehicles for remote-controlled tumor targeting, bioimaging and chemotherapy both *in vitro* and *in vivo* [56].

Other than upconversion photorelease of drugs, some studies have utilized UCNCs for imaging molecules for remote controlled optical bioanalysis in complex living systems. In this regard, Xing et al. reported a system for upconversion photocontrolled uncaging of D-luciferin and subsequent bioluminescence imaging *in vitro* and *in vivo* (Fig. 2B) [51]. In other cases, Li et al. introduced a novel UCL-activated DNA nanodevice for spatiotemporal controlled ATP [147], miRNAs [148] sensing in living cells and mice.

3.1.3. Prodrug activation

In addition to photorelease of encapsulated drug molecules, upconversion nanoplatforms have also widely applied in the development of NIR photoactivatable anticancer prodrugs (e.g. cisplatin derivatives). Lin et al. designed a stable and multifunctional drug delivery system by combing UCNPs with the nontoxic cisplatin (IV) prodrug [63]. After NIR laser treatment, the imaging-guided remote photorelease of cytotoxic cisplatin (II) could not only effectively kill cancer cells but also reduce the drawbacks of cisplatin including the limited cellular uptake, poor pharmacology, fast blood clearance and severe kidney toxicity and neurotoxicity. Besides, Xing et al. developed another upconversion photoactivatable Pt(IV)-based prodrug (Fig. 3A), this nanosystem allowed remote control of antitumor platinum (IV) prodrug activation and simultaneously real-time imaging of activated Pt (II) drug-induced cells apoptosis [61]. To validate the therapeutic action *in vivo*, Lin et al. also applied such upconvertion photocontrolled trans-platinum(IV) prodrugs for the inhibition of tumor growth in mice [62].

In addition to the design of UCNPs/platinum complex-based prodrugs, other commonly used cancer chemotherapeutic drugs have been developed into NIR photoactivatable prodrugs. For instance, aforementioned UCNPs/DOX covalently linked nanoconjugates were capable of NIR laser-triggered release of free drug molecules [53]. Li et al. reported UCNPs/chlorambucil based nanoplatforms that were

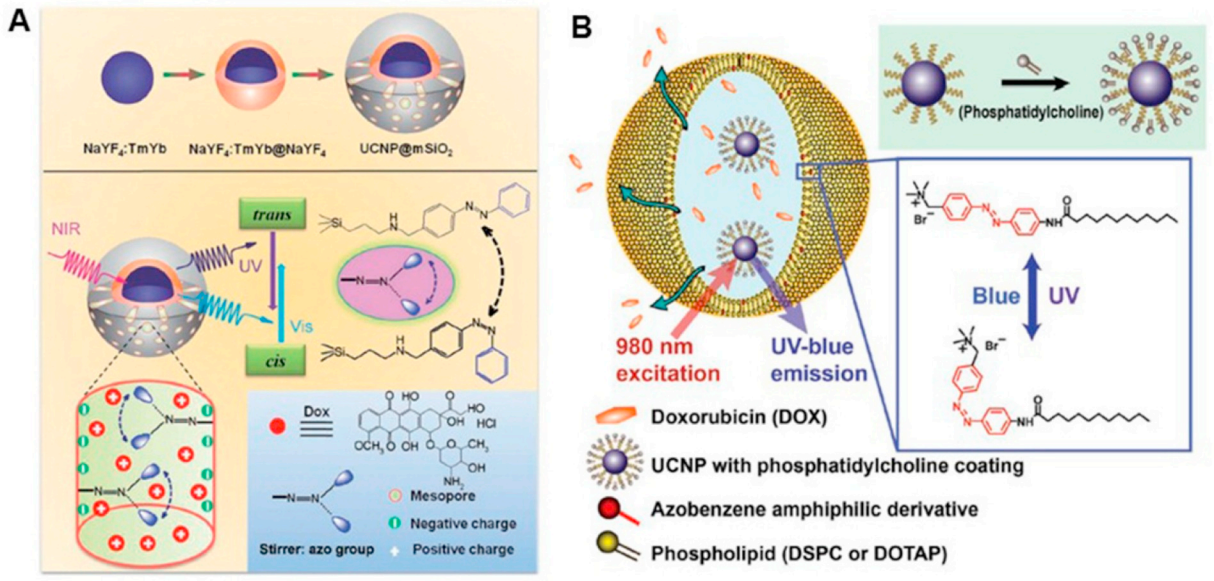

Fig. 4. Representative UCNCs for upconversion photoisomerization-triggered drug delivery. (A) NIR light-triggered DOX release by making use of the upconversion property of UCNPs and trans–cis photoisomerization of azo-molecules grafted in the mesopore network of a mesoporous silica layer Reprinted with permission [80]. Copyright 2013, Wiley-VCH. (B) NIR-triggered azobenzene-liposome/UCNPs hybrid vesicles for photocontrolled drug delivery. Reprinted with permission [81]. Copyright 2016, Wiley-VCH.

successfully achieved NIR-regulated drug release in the living animals (Fig. 3B) [60]. Krull et al. fabricated a UCNPs/5-fluorouracil (5-FU) nano-prodrug system for targeted and NIR photocontrolled tumor therapy (Fig. 3C) [58].

3.2. Upconversion photoisomerization for therapeutics release

Structural or conformational switching in the nanocarriers undergoes a physical change upon light irradiation that is also feasible for photocontrolled therapeutics release. In this line, Shi et al. reported an azobenzene-modified upconversion nanocarrier for NIR light-triggered anticancer drug release (Fig. 4A) [80]. Upon 980 nm laser excitation, the photoresponsive azobenzene molecules in the pore network of the mesoporous silica layer enabled reversible photoisomerization with a continuous rotation–inversion movement, such back and forth wagging motion acting as a molecular impeller that propelled the release of DOX in tumor cells. Another upconversion photoisomerization-based liposome system developed by Zhang et al. has allowed NIR photocontrolled anticancer drug delivery *in vitro* and in living animals (Fig. 4B) [83]. The hybrid azobenzene liposome vesicles encapsulated with UCNPs and DOX demonstrated reversible isomerization capability caused by simultaneous UV and visible light emitted from the UCNPs, which subsequently induced liposomes dialysis and therefore realizing the photocontrolled drug release. Compared with normal liposome-based drug release through passive and random molecules leakage, such photocontrolled liposome platforms achieved both enhanced therapeutically effective drug accumulation, and reducing the side effects of drugs on normal tissues.

Additionally, upconversion photoisomerization nanoplatforms have also widely used in various biomolecules photorelease. For example, Gong et al. developed UCNP-based siRNA nanocarriers for NIR-controlled gene silencing [82]. In which, siRNA was capped onto UCNPs surface through the azobenzene (Azo)–cyclodextrin (CD) host–guest interaction. The NIR-to-UV emission effectively triggered the trans-to-cis photoisomerization of azobenzene, leading to the photorelease of siRNA through unmatched host − guest pairs. Qu et al. constructed DNA-mediated and spiropyran (SP)-modified hollow UCNCs for protein harvesting and cellular release [84]. In this system, the negatively charged proteins harvesting could be achieved through the electrostatic interactions *via* the positively charged merocyanine (MC)-functionalized UCNCs. After NIR light exposure, the MC structure converted to the neutral SP and thereby releasing of the trapped proteins. Overall, upconversion-triggered photorelease techniques significantly overcome the disadvantages (e.g. phototoxicity and low tissue penetration) encountered in conventional UV/Vis light-mediated delivery systems, providing opportunities for further biomedical translation research.

3.3. Upconversion photoactivation for optogenetics

In recent years, the utilization of UCNPs for classical optogenetic activation has provided great opportunities for NIR manipulation of neuronal or non-neuronal functions [149,150]. Moreover, upconversion optogenetics allow highly spatial and temporal control of biological signaling pathways both *in vitro* and in deep tissues. So far, various optogenetic tools with different chromophores-based photo-actuators are developed (Scheme 4). These light-sensitive systems including microbial light-gated ion channels (channelrhodopsins, ChRs) and other soluble photoreceptor proteins that have enabled specific regulation of biomolecular reactions localized in the cell membrane, cytoplasm and nucleoplasm [151]. In light with the large anti-stokes shift and multi-color-turning capabilities of UCL, current progresses of UCNPs-mediated optogenetics have achieved precise photocontrol of neuronal excitability, behaviors, immunomodulation and tumor phototherapy. Some reviews have discussed the basic design principle and recent applications of upconversion optogenetics [152–154]. Therefore, in this section we mainly highlight the technical improvements of UCNPs functionalization and representative NIR optogenetic manipulations *in vivo*.

The recent advances of upconvertion optogenetic studies have been briefly summarized in Table 1 (the part of photoactivation). Other than some initial photoactivations of ChRs in cells, the first proof-of-concept utilization of UCNPs for optogenetic regulation in living animals was reported by Zhou and Han et al. in 2015 [85]. Blue emissive core-shell UCNPs were subsequently modified with PAA and streptavidin antibody, such Stv-UCNPs specifically bounds to engineered ORAI1 channels in the plasma membrane. Upon 980 nm light irradiation, the

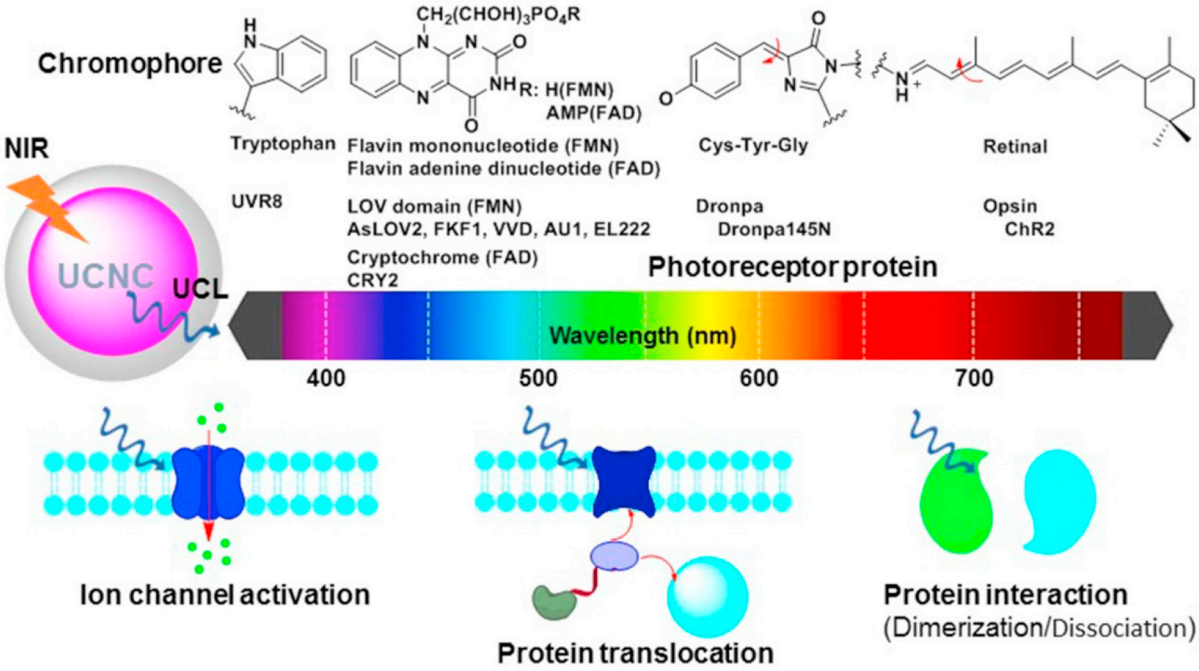

Scheme 4. NIR upconversion optogenetics with representative chromophores of photoreceptor proteins. Chemical structures are reprinted with permission [151]. Copyright 2008, American Chemical Society.

optogenetic system (termed "Opto-CRAC") can be selectively activated, subsequent Ca^{2+} influx enabled downstream signaling effectors expression, further affecting the immune-inflammatory responses. Additionally, such a NIR optogenetic platform was used for *in vivo* immunomodulation and photoactivated cancer immunotherapies. This study not only demonstrated the feasibility of guiding NIR light for confining localized and deep-tissue optogenetic modulation, but also showed the possibility to activate other optogenetic tools (e.g., ChR2 and CRY2). In another pioneer study, Xing et al. achieved membrane localized optogenetic activation of ChR2 *via* glycan metabolic covalent-labeling strategy, in which Nd-sensitized core-shell UCNPs were coated with PAA polymer and conjugated with DBCO moiety for Cu-free click chemistry [91]. With 808 nm laser excitation, Ca^{2+} influx effectively triggered apoptosis occurrence in Hela cells. Furthermore, such a system demonstrated the applicability for Ca^{2+} signaling pathway activation in zebrafish.

Besides, some representative UCNPs-ChRs based studies have realized NIR-mediated behaviors manipulation. For example, Zhang et al. developed quasi-continuous wave 980 nm laser excitation approach to improve the efficacy of optogenetic neuromodulation in ChR2-expressed *C. elegans* [87]. This work further achieved remote photocontrol of touch-akin reversal behavior of *C. elegans*. Recently, Gao et al. engineered 808 nm excited and green-emissive UCNPs for the optogenetic manipulation of the motor behaviors in *C. elegans* with Chrimson-expressing [98]. Furthermore, NIR optogenetic control of behaviors has also been realized in living animals. Shi et al. reported UCNPs-based implantable micro-devices that can multiplexed optogenetic control of neurons expressing opsin proteins (ChR2 or C1V1) in rat brain [93,94]. The NIR illumination was capable of reaching specific brain stimulation in different regions, which allowed complex activation or silencing brain functions and even behaviors modulation.

To further improve the efficacy of optogenetic neuronal inhibition, core-shell-shell UCNPs-based fully implantable upconversion devices with almost three-fold enhancement of UCL intensity were designed and used for the excitation of halorhodopsin (eNpHR, a photosensitive Cl^- channel) *in vitro* and in mice [96]. To minimize the invasiveness and diversify the applicability, McHugh and Liu et al. injected UCNPs in mice brain and realized NIR deep-neurons regulation for remote therapy of neurological diseases, the optogenetic-mediated seizure silence through inhibition of hippocampal excitatory cells enabled memory recall [97].

UCNPs were also utilized in other non-ion-channel based optogenetic modulation. Among them, Chang et al. constructed versatile upconversion nanosystems for optogenetic modulation of a heterodimerization module (Cry2-FADD/Cib-Fas) [100]. This study indicated that deeply penetrating NIR light could be used to activate the apoptotic signaling *in vitro* and *in vivo*, providing great potential for tumor phototherapy.

3.4. Upconversion photosensitization for photodynamic therapy

3.4.1. UCNCs for antitumor PDT

Photosensitization mediated cytotoxic singlet-state $^1O_2$ or other reactive oxygen species (ROS) generation has been used as a clinical treatment modality against tumor and microbial infections, which is also termed photodynamic therapy (PDT) [155]. In PDT, light, oxygen and photosensitizer (PS) are three major components, where light-triggered PS molecules excitation leads to energy transfer to neighboring O_2 or other substrates, generating ROS and subsequently inducing cells damage [156,157]. Such a paradigm has high therapeutic precision and efficiency, but less invasiveness and side effects in the comparison with that of commonly used chemo- and radio-therapy. However, owing to most PS molecules can only be sensitized by visible or even UV light, traditional PDT has difficulty in the practical treatment of tumors and other diseases in deep tissues. Recently, UCNPs have received considerable attention for bioimaging and biosensing owing their unique NIR photon-upconverting features, which also provide unprecedented opportunities for the realization of tissue-penetrable NIR light-triggered PDT [158,159].

To build UCNPs-based PDT platforms, those widely used organic or inorganic PS molecules need to be loaded onto UCNCs thereby allowing effective photosensitization. Generally, there are several common approaches to functionalize UCNCs as nanocarriers compromising silica encapsulation, polymers (PEG, PAA, PEI, PVP, chitosan and dextran

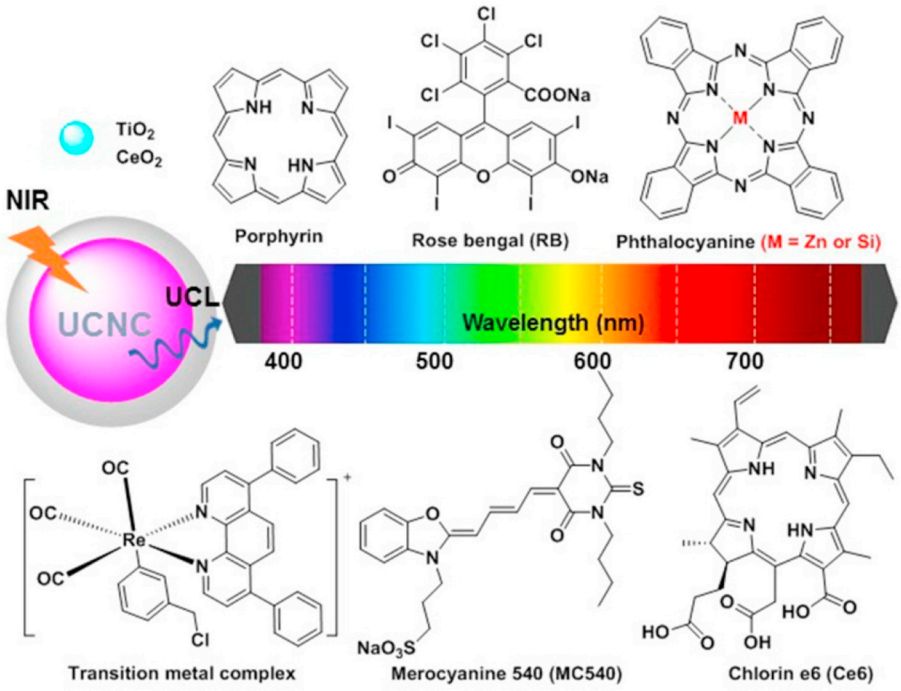

Scheme 5. UCNCs with representative photosensitizers for NIR photodynamic therapy.

etc.) encapsulation and covalent conjugation. To improve the efficacy of upconversion PDT, core-shell or core-shell-shell nanostructured UCNCs with enhanced UCL were also developed.

As summarized in Table 1 (the part of photosensitization), with the integration of multicolor emissive UCNPs and appropriate PS molecules, various flexible upconversion PDT studies have been reported and applied for antitumor treatment *in vitro* and *in vivo*. Conventional UV or visible light-sensitive PS molecules like phthalocyanines (Pc), porphyrins, transition metal complexes, metal oxide nanoparticles (MO NPs, e.g. TiO_2, CeO_2) and so on have been fabricated with UCNCs (Scheme 5), which can be excited by either 980 nm or 808 nm laser. For example, Zhang et al. developed mesoporous-silica ($mSiO_2$) coated UCNCs with zinc (II) phthalocyanine (ZnPc) loading for NIR PDT study [101]. Moreover, such a nanoplatform was further engineered with targeting ligand folic acid (FA) and dual PS molecules (MC540 and ZnPc) to fit both UCL_{540} and UCL_{660} spectra, achieving high precise, effective and noninvasive deep-melanoma-cancer therapy in living animals [102].

In addition, the representative porphyrin-based PS molecule chlorin e6 (Ce6) has also been widely conjugated with polymer modified UCNCs for PDT applications. Among them, Liu et al. loaded Ce6 in PEGylated UCNCs *via* hydrophobic interactions, the PDT study *in vivo* achieved enhanced treatment efficacy for tumors blocked by thick biological tissues [113]. Another similar work reported by Hyeon et al. also developed the UCNC-Ce6 system for simultaneous tumor imaging and PDT in mice [110]. Furthermore, metal-organic framework (MOF) as an emerging nanosystem has received intensive attention for upconversion PDT research. MOFs can keep the PS molecule as a monomer and prevent from self-quenching, which possess a remarkable feature to solve solubility and aggregation issues in the PDT process. Some UCNP-porphyrin-based MOFs have been reported in recent years, for example, Yan et al. introduced heterodimers composed of porphyrinic nanoscale MOF and UCNPs for NIR-induced PDT [120]; Very recently, Zhao et al. constructed a similar Janus MOF nanostructure with porphyrin and 808 nm-excited UCNPs for amplified PDT against cancer [112].

Rose bengal (RB) derivatives were also widely used as PS molecules that can be covalently conjugated on polymer-modified UCNCs, such a covalent conjugating strategy achieved high PS loading efficacy and luminescence resonance energy transfer (LRET) yields. Zhang et al. introduced this highly efficient 980 nm laser photosensitizing nanoconjugates for simultaneous PDT and tumor imaging *in vitro* [122]. Then Yan et al. constructed Nd-sensitized UCNPs with convenient RB conjugation for effective photodynamic inhibition of tumor growth and metastasis in mice models through 808 nm laser irradiation [115].

Besides, some transition metal complexes and metal oxide NPs have also been fabricated with UCNPs for NIR PDT applications. Different from the loading strategies as mentioned above, Zhang et al. reported an approach by uniformly coating photocatalyst TiO_2 on UCNPs surface, this thin and continuous TiO_2 layer showed good stability in the process of PDT both *in vitro* and *in vivo* [132]. At the same time, Lin et al. introduced an efficient UCNPs@TiO_2 based core/shell nanoplatform for NIR light mediated PDT [131]. Similar to TiO_2, cerium oxide (CeO_2) NPs have also been recently utilized as novel PS structures in upconversion PDT [30,138,139]. In which, CeO_2 nanostructures were either directly coated or loaded on the surface of UCNPs, serving as NIR light-sensitive photocatalyst. In particular, CeO_2 can act as a catalase with the ability of reversibly switching from Ce^{4+} to Ce^{3+} thereby converting H_2O_2 to H_2O and O_2 [160], which enabled O_2-evolution with enhanced efficiency of PDT.

There are also some studies engineered different types of photosensitizing UCNCs for tumor PDT. For example, Liu et al. prepared conjugated polyelectrolyte (CPE) encapsulated UCNCs for both anticancer drug loading and PDT applications [140]; Khaydukov et al. reported an endogenous photosensitizer Riboflavin (Rf, a vitamin) based upconversion nanosystem [143]; Zvyagin et al. developed KillerRed fluorescent protein conjugated UCNC for deep-penetrating PDT treatment [145].

3.4.2. UCNCs for antimicrobial PDT

Other than the application in tumor phototherapy, UCNCs have also been widely applied for antimicrobial therapeutics as summarized in Table 2. Similar to the antitumor UCNCs, various antimicrobial PDT platforms were constructed by attaching appropriate photosensitizers on the surface of functionalized UCNPs. Besides, some earlier reported that UVC-emissive upconversion systems have also achieved effective antibacterial actions [161,162]. These studies demonstrated that the

Table 2
Representative UCNCs for photodynamic antibacterial therapy.

UCNCs	Ex. / Em[a]	Power density[b]	Applications[c]	Ref
$NaYF_4$:Yb/Er@$NaGdF_4$@SiO_2@Rose bengal	980 nm / 540, 650 nm	1 W/cm^2	Anti-MRSA and ESBL-producing *E. coli* strains in vitro	[163]
$LiYF_4$:Yb/Er@β-carboxyphthalocyanine zinc@PVP	980 nm / 540, 650 nm	0.5 W/cm^2	Anti-infectious against MRSA and MDR *Escherichia coli*; antifungal effect against *Candida albicans*	[164]
$NaYF_4$:Yb/Er@mSiO_2/SiPc	976 nm / 540, 650 nm	0.4 W/cm^2	Antimicrobial photodynamic therapy against *E coli* and *S. aureus*	[165]
$NaYF_4$:Yb/Tm@PEI@ Curcumin	980 nm / 480 nm	0.5 W/cm^2	Anti-MRSA in vitro and in periprosthetic joint infection mice	[166]
$NaYF_4$:Yb/Er@mSiO_2/Ce6	980 nm / 540, 650 nm	-	Antimicrobial PDT against *P. gingivalis, P. intermedia* and *F. nucleatum*	[167]
$NaYF_4$:Yb/Er@$NaGdF_4$:Nd@mSiO_2/Rose Bengal/AgNPs	980 nm / 540, 650 nm	2 W/cm^2	PDT against MRSA in vitro	[168]
$NaYF_4$:Yb/Tm@PVP@TiO_2	980 nm / 365, 480 nm	2.5 W/cm^2	PDT against periodontitis-related pathogens, *S. sanguinis*, *P. gingivalis* and *F.nucleatum*	[169]
$NaYF_4$:Yb/Er/Nd@$NaYF_4$:Nd@TiO_2:Mn	808 nm / 540, 650 nm	-	Photocatalytic antibacterial therapy against *B. subtilis and E coli*	[170]
$NaYF_4$:Yb/Er@AuNP@SiO2@D-TiO_2	980 nm / 540, 650 nm	0.68 W/cm^2	Photocatalytic inactivation of *E coli* and MRSA *in vitro*	[171]

[a] Excitation wavelength and major upconversion luminescence (UCL) wavelengths.
[b] NIR excitation power density.
[c] MRSA, methicillin-resistant *Staphylococcus aureus*, MDR, multidrug resistance; ESBL, extended spectrum β-lactamase.

NIR photocatalytic UCNCs not only exhibited good therapeutic effects against both gram-positive and gram-negative bacteria, but also showed good promise for the treatment of infectious disease caused by antibiotic-resistant (or multidrug resistant, MDR) bacteria.

4. Synergistic upconversion photocontrolled therapy

Owing to the remarkable superadditive therapeutic effects, the modern nanotechnology-assisted multimodal synergistic therapy that simultaneously blocks multiple pathological mediators, providing new opportunities for the treatment of complex diseases [172]. With the unique optical properties, UCNPs have been theoretically designed as multifunctional phototherapeutics for realizing bimodal and even trimodal synergistic therapy. In particular, some representative upconversion multimodal therapeutics have shown great potential in improving antitumor effects and overcoming multidrug resistance. In this section, featured design strategies and applications of UCNCs-based synergistic therapeutic nanoplatforms will be discussed in detail.

4.1. Chemotherapy/gene therapy

Combination of chemotherapy and siRNA-based gene therapy has gained researcher's attention to overcome chemoresistance in the tumor treatment. Lin et al. reported an effective UCNC-carrier system loaded with both eukaryotic translation initiation factor 4E (eIF4E) siRNA and Pt (IV) prodrug [173]. After cancer cells uptake, siRNA can be released selectively in the low pH tumor microenvironment, which can silence the target gene, protein expression thereby conferring cisplatin resistance. Meanwhile, Pt (IV) prodrug can be reduced effectively to cisplatin through reducing agents such as ascorbic acid and glutathione in the tumor cells, enabling specific DNA damage. In this way, the eIF4E siRNA has sensitized and enhanced the platinum based tumor chemotherapy.

4.2. PDT/chemotherapy

Another synergistic antitumor phototherapy approach has been developed by the combination of NIR upconversion-mediated PDT and chemotherapy. In this case, Liu et al. fabricated upcoversion nanoplatforms with conjugated polyelectrolyte (CPE) as the photosensitizer, as well as a nanocarrier for chemotherapeutic drug DOX loading through an UV-cleavable ortho-nitrobenzyl (NB) linker (Fig. 5A) [140]. Upon 980 nm laser irradiation, the up-converted UV emission enabled photo-regulated DOX release, while the up-converted visible light initiated the polymer photosensitizer to produce ROS for PDT. Such a synergistic PDT and photochemotherapy platform not only achieved simultaneously spatial/temporal controlled and on-demand therapeutic photorelease, but also showed enhanced anticancer effects.

In addition, Shi et al. designed double silica-shelled UCNCs that were capable of co-delivering the photosensitizer molecules and a bioreductive pro-drug (tirapazamine, TPZ) for treating hypoxia tumors both *in vitro* and in mice model [106]. Qu et al. prepared Ce6 and DOX co-loaded UCNCs that also showed effective NIR-triggered synergistic anti-tumor performances (Fig. 5B) [114].

4.3. PDT/gene therapy

Compare with traditional chemotherapy-based multimodal therapeutic systems, the combination of PDT with siRNA therapy has become an alternative strategy in cancer treatment with enhanced anticancer efficacy and relatively low side effects. In this regard, Liu et al. synthesized multilayer polymer coated UCNCs, and then loaded simultaneously with Ce6 and Plk1 oncogene-targeted siRNA (Fig. 6A) [112]. The NIR laser-mediated PDT and siRNA delivery induced significant cancer cell apoptosis. Such combined PDT and gene therapy remarkably enhanced cancer cell killing effects.

Fan et al. reported the photo-induced charge-variable cationic

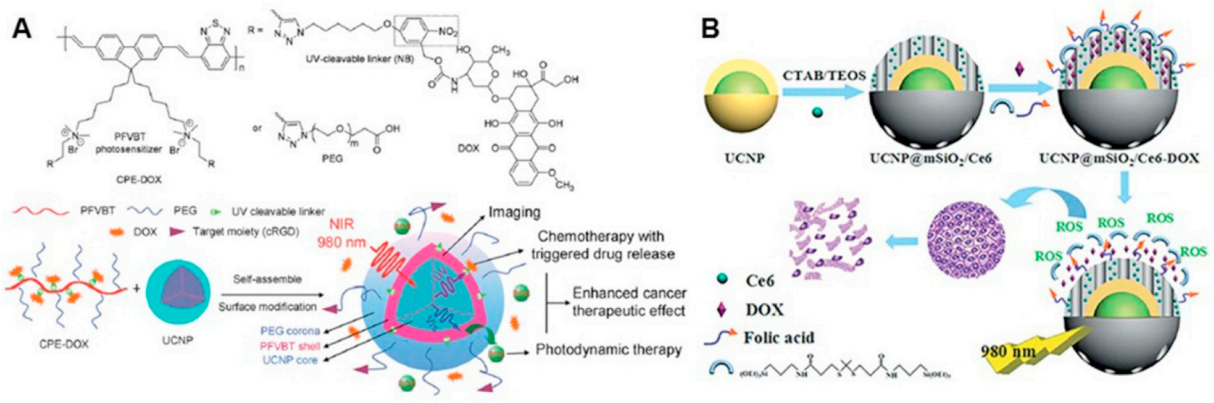

Fig. 5. Representative UCNCs for synergetic tumor PDT and photochemotherapy. (A) NIR laser regulated initiation of the photosensitizer to generate ROS for PDT and on-demand photorelease of covalently linked DOX for tumor chemotherapy. Reprinted with permission [140]. Copyright 2014, The Royal Society of Chemistry. (B) NIR light triggered PDT and photo-responsive release of encapsulated DOX for tumor chemotherapy. Reprinted with permission [114]. Copyright 2016, Wiley-VCH.

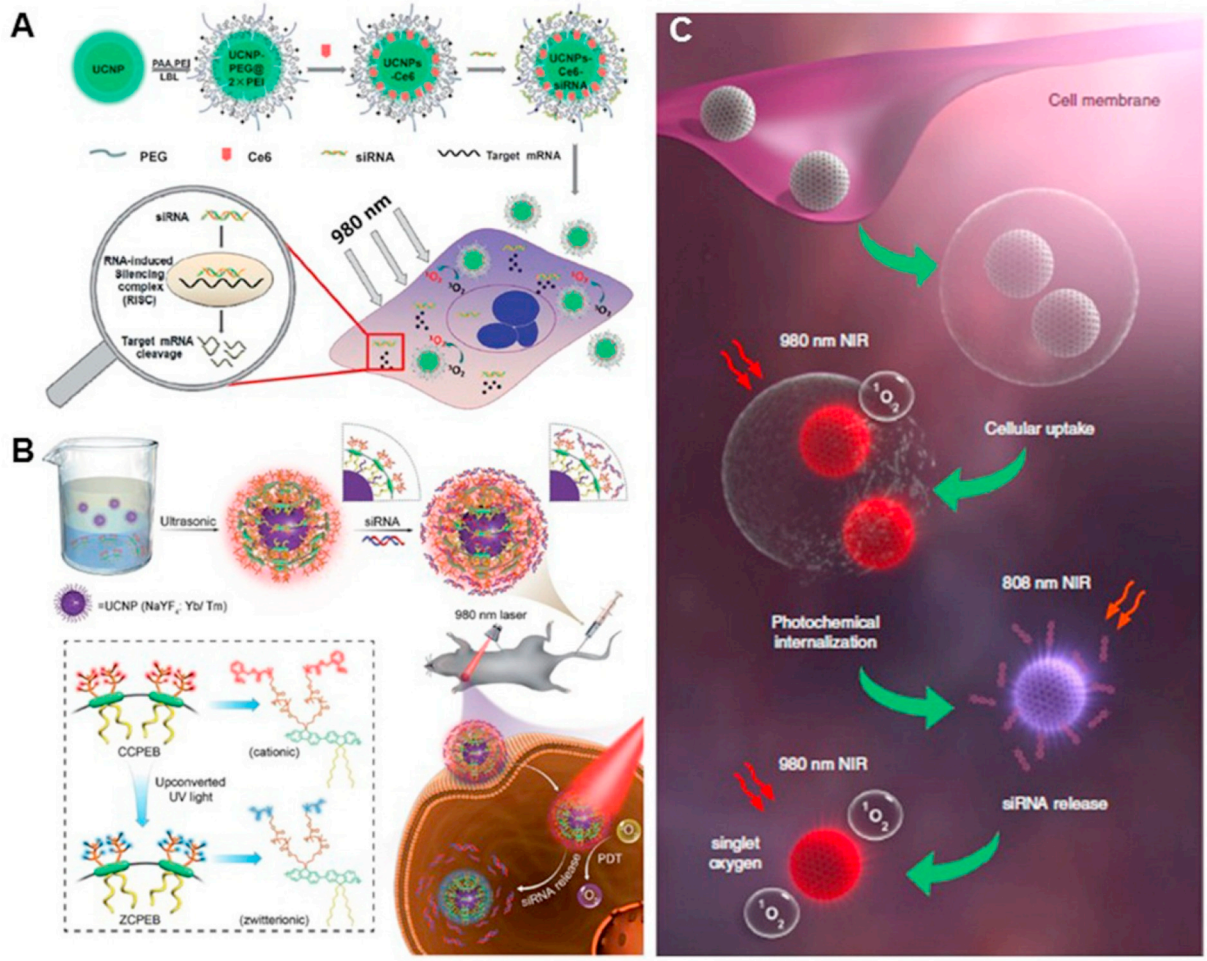

Fig. 6. Representative UCNCs for synergetic tumor PDT and gene therapy. (A) Polymers functionalized UCNPs for co-loading of Ce6 and siRNA, and then applied for the combined tumor PDT and gene therapy. Reprinted with permission [112]. Copyright 2014, The Royal Society of Chemistry. (B) NIR light triggered PDT and photo-responsive release of encapsulated DOX for tumor chemotherapy. Reprinted with permission [141]. Copyright 2017, Wiley-VCH. (C) Orthogonally excited and Azo-$mSiO_2$-modified UCNCs for programmable photoactivated tumor PDT and gene therapy. Reprinted with permission [108]. Copyright 2019, Nature Publishing Group.

conjugated polyelectrolyte brushes (CCPEB) encapsulated UCNCs for promoted siRNA release and collaborative PDT under NIR light irradiation (Fig. 6B) [141]. Consequently, this synergistic PDT and gene therapy towards tumor showed good therapeutic effect in living mice. Very recently, Zhang et al. prepared orthogonal (980/808 nm) photoactivable UCNPs and used for programmed photoactivation of multiple therapeutic processes (e.g. PDT and gene delivery) with improved efficacy (Fig. 6C) [108]. After precise photocontrolled endosomal escape through photochemical-internalization, followed by photoregulated gene knockdown of superoxide dismutase-1 to increase ROS sensitivity, such sequential activated PDT demonstrated significantly higher therapeutic efficacy *in vitro* and *in vivo* in comparison to conventional, non-

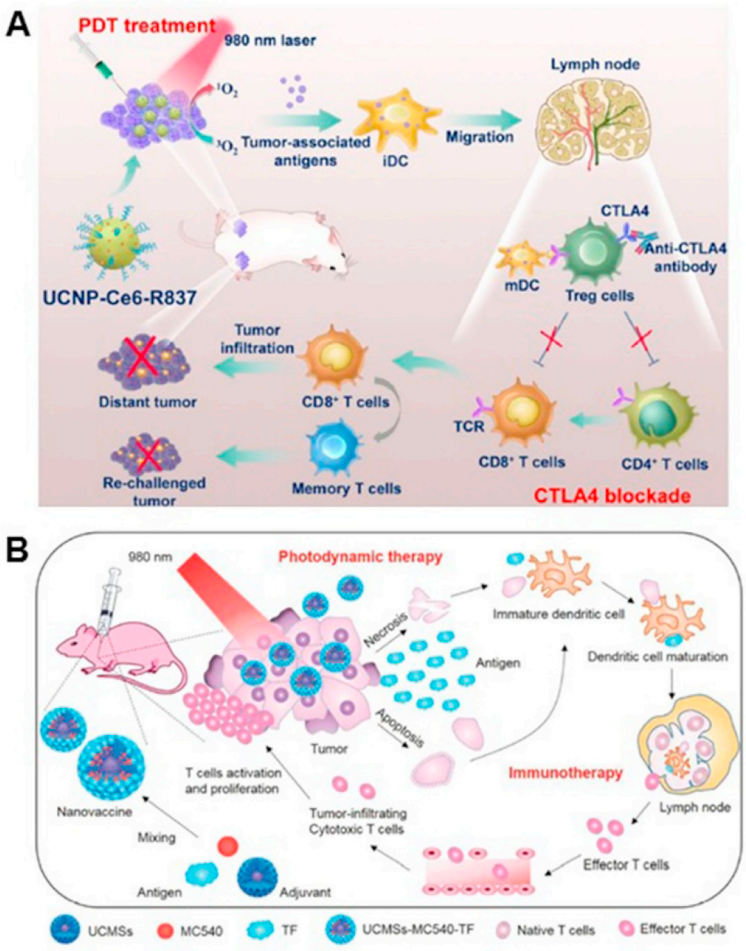

Fig. 7. Representative UCNCs for synergetic tumor PDT and immunotherapy. (A) The illustration of combining NIR-mediated PDT with CTLA-4 checkpoint blockade for cancer immunotherapy. Reprinted with permission [115]. Copyright 2017, American Chemical Society. (B) Fabrication and mechanism of UCMSs–MC540–TF nanovaccines for photodynamic immunotherapy. Reprinted with permission [144]. Copyright 2018, Wiley-VCH.

programmed PDT/gene therapy systems.

4.4. PDT/immunotherapy

It has been recognized that PDT shows the ability to potentiate checkpoint blockade and trigger antitumor immune responses by producing tumor-associated antigens [174]. In this aspect, Liu et al. reported a strategy with UCNP-based PDT in combination with immunotherapy, in which the photosensitizer Ce6, and imiquimod (R837), a Toll-like-receptor-7 agonist were simultaneously loaded (Fig. 7A) [115]. Such a multitasking nanoplatform enabled NIR-triggered effective photodynamic destruction of tumors, and generating a pool of tumor-associated antigens in the presence of R837, which were able to promote strong antitumor immune responses. Consequently, PDT in combination with the cytotoxic tlymphocyte-associated protein 4 (CTLA-4) checkpoint blockade not only showed enhanced efficacy in tumors elimination exposed to the NIR laser, it but also induced strong antitumor immunities to suppress the growth of distant tumors left behind after PDT treatment.

Lin et al. also reported another strategy using the photosensitizer MC540, model proteins (chicken ovalbumin (OVA)), and tumor antigens (tumor cell fragment (TF)) encapsulated upconversion nanovaccines for PDT-enhanced tumor immunotherapy (Fig. 7B) [144]. Under 980 nm light irradiation, the strongest Th1 and Th2 immune responses and the highest frequency of $CD4^+$, $CD8^+$, and effector-memory T cells validated the best synergistic immunopotentiation action. Additionally, this nanosystem showed more effective inhibition of tumor growth and increasing the survival of colon cancer (CT26)-tumor-bearing BALB/c mice compared with either PDT or immunological therapy alone, suggesting the potential of such nanovaccines as immunoadjuvants for clinical cancer immunotherapy.

4.5. PDT/PTT/chemotherapy

Besides, Yang et al. deigned a tri-modal photodynamic-/photothermal-/chemo-therapy derived synergistic antitumor nanoplatform [107]. The photosensitizer ZnPc, photothermal agent conjugated CDs- P (NIPAm-MAA) and chemotherapy drug DOX were co-encapsulated in mesoporous silica coated UCNCs, achieving an efficacious tumor inhibition effect both *in vitro* and *in vivo*.

5. Bioimaging-guided precise upconversion phototherapy

Based on the intrinsic luminescent properties of UCNPs, upconversion-based nanotheranostics not only allows photocontrolled multimodal therapy mentioned above, but also provides great promise for disease sensing and imaging-guided remote intervention. Some representative upconversion bioimaging and combined tumor phototherapy studies have been reported in recent years.

5.1. UCL-guided therapy

Yeh et al. applied UCNCs as the NIR-triggered targeting and drug delivery vehicles that could be used for deep-tissue photocontrolled targeting, bioimaging, and chemotherapy (Fig. 8) [56]. Briefly, the

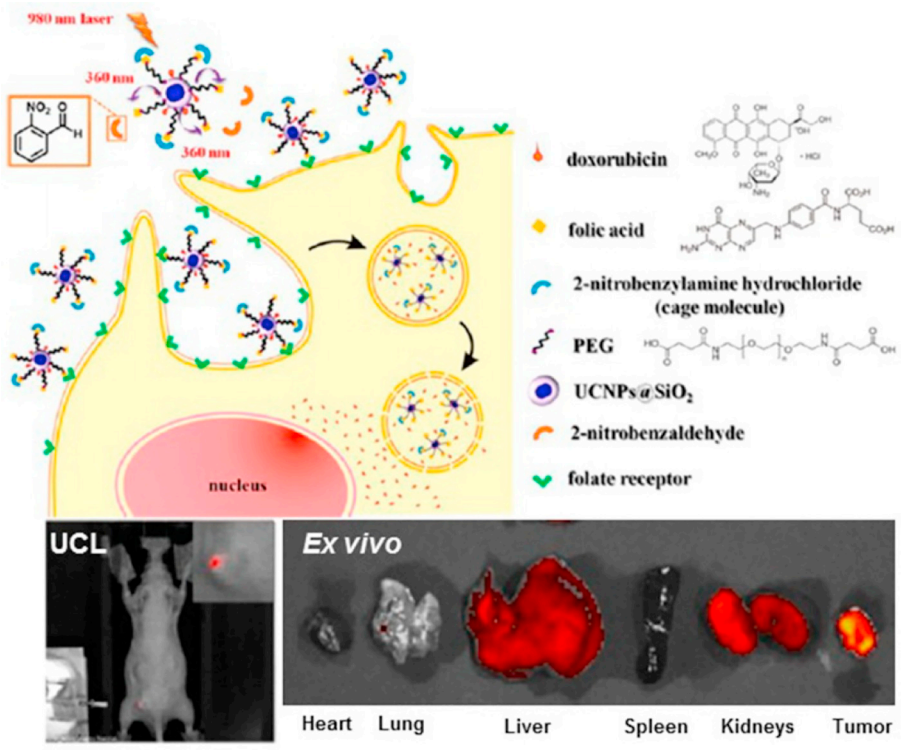

Fig. 8. UCL imaging-guided tumor therapy. Reprinted with permission [56]. Copyright 2013, American Chemical Society.

upconverting UV emission (360 nm) mediated photocleavage of the protecting group (ONB) enabled selective release of DOX through breaking disulfide bond in lysosomes. Moreover, UCL imaging *in vitro* and *in vivo* validated the effective tumor accumulation and precise chemotherapeutic efficacy.

Besides, UCL imaging-guided simultaneous PDT under the same NIR light irradiation has also widely applied in tumor phototherapy. For example, Zhang et al. introduced a multifunctional and FA-modified upconversion nanoplatform with the photosensitizer RB conjugation for effective image-guided cancer cells killing [175]. Gu et al. developed tumor targeted FASOC-UCNP-ZnPc nanoconstructs that demonstrated remarkable photocontrolled therapeutic efficacy against deep-seated tumors *in vivo* [176]. Very recently, Zhang et al. reported NIR excited orthogonal emissive UCNCs with the photosensitizer ZnPc encapsulation that were capable of NIR light-triggered and targeted tumor photoablation under spatiotemporal control [109].

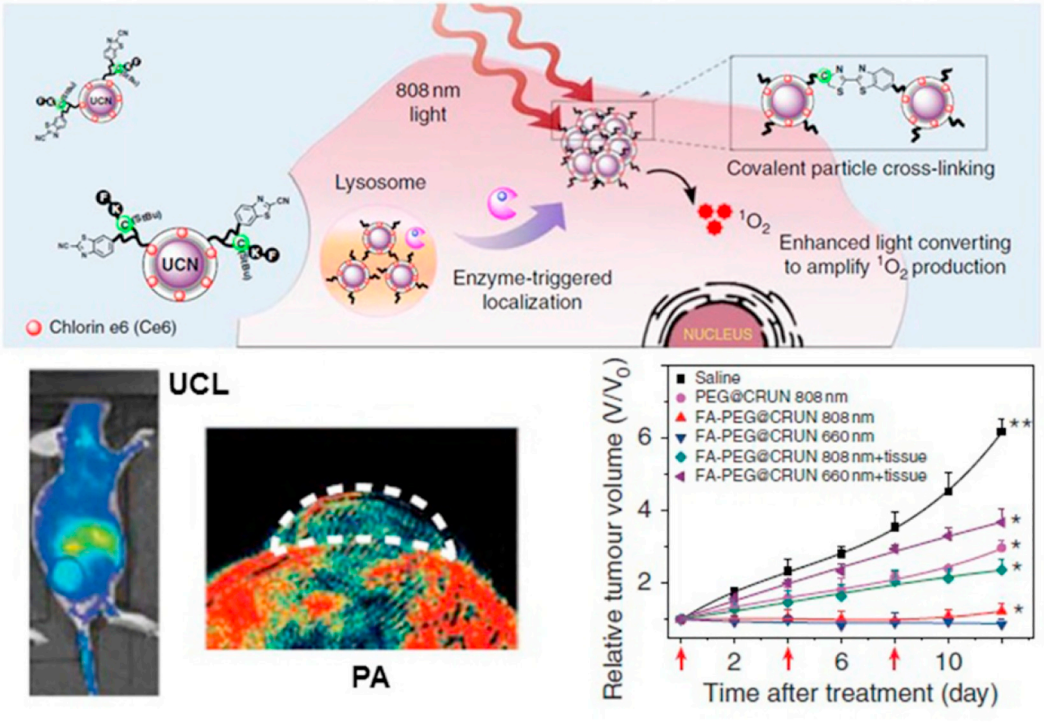

Fig. 9. UCL and PA imaging-guided photodynamic tumor therapy. Reprinted with permission [116]. Copyright 2016, Nature Publishing Group.

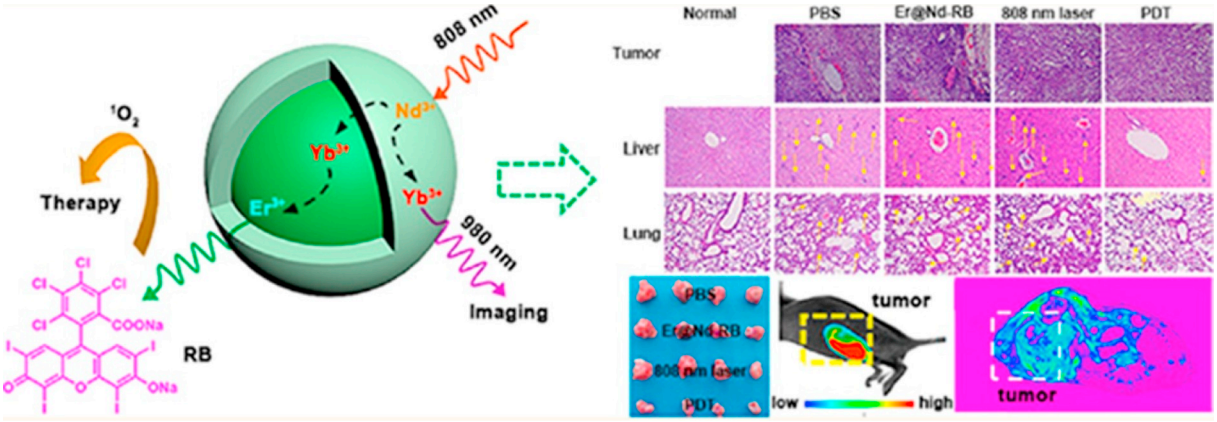

Fig. 10. UCL/MRI imaging-guided tumor therapy. Reprinted with permission [124]. Copyright 2016, American Chemical Society.

5.2. UCL/PA-guided therapy

Additionally, Xing et al. developed a microenvironment-sensitive phototheranostics for remotely monitoring tumor localization through UCL/photoacoustic (PA) imaging, and meanwhile achieving effective PDT (Fig. 9) [116]. Typically, the peptide-modified and Ce6-conjugated upconversion nanosystem could be selectively cleaved by tumour-specific cathepsin protease, this reaction induced covalent cross-linking

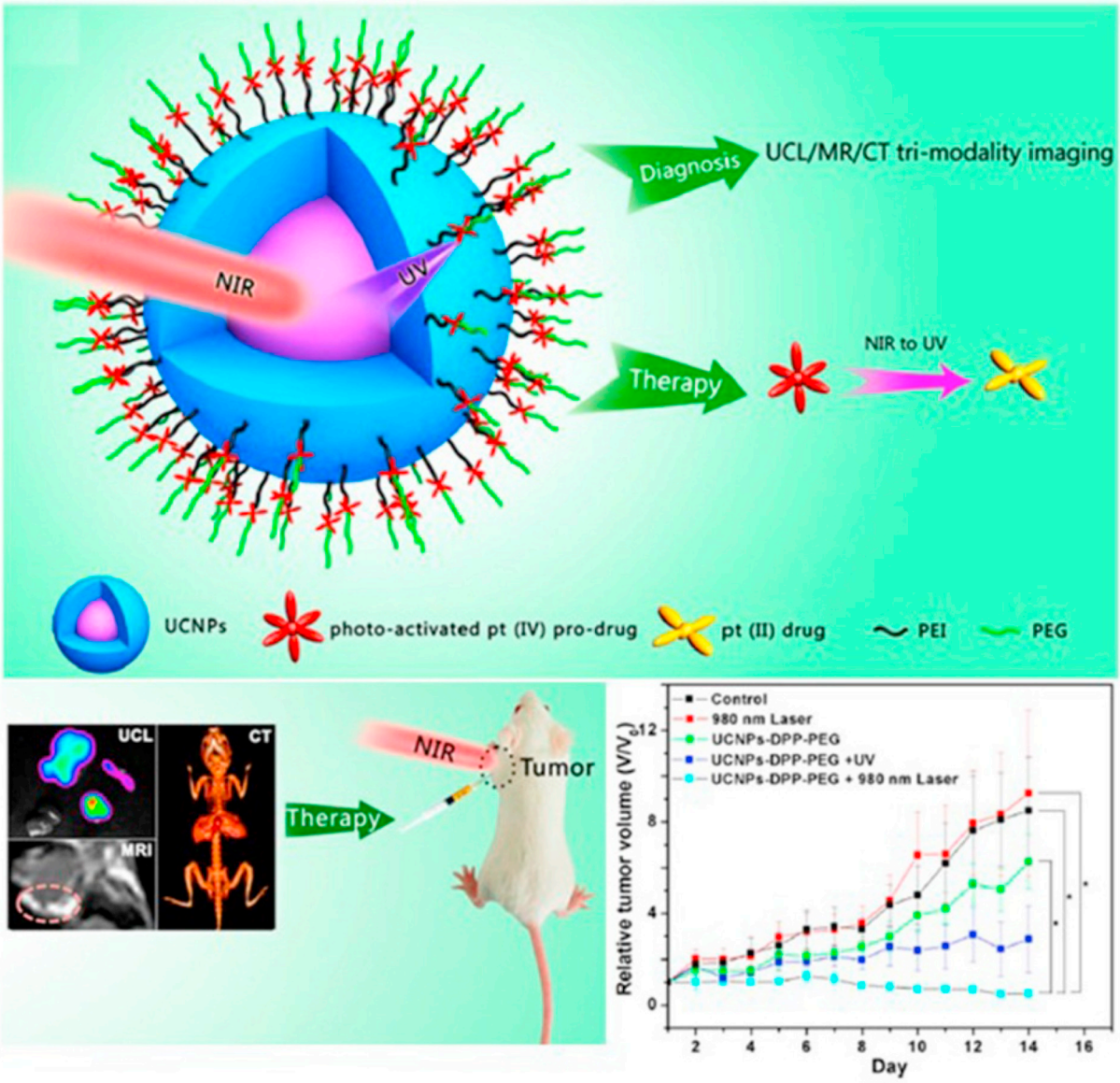

Fig. 11. UCL, MRI and CT imaging-guided tumor photochemotherapy [62]. Reprinted with permission. Copyright 2016, Wiley-VCH.

between the exposed cysteine and 2-cyanobenzothiazole on neighbouring nanoparticles, thus triggering the accumulation of theranostic agents within the tumor area. Upon 808 nm laser irradiation, the cross-linked nanoplatorm showed enhanced UCL and PA intensities which further enabled the amplification of ROS generation for tumor PDT *in vitro* and in mice.

5.3. UCL/MRI-guided therapy

Besides serving as luminescent imaging agents and therapeutic carriers, some UCNCs with Gd^{3+} or Mn^{2+} ions also exhibit the capability of magnetic resonance imaging (MRI). Yan et al. developed an effective upconversion nanotheranostic system ($NaGdF_4$:Yb/Er@$NaGdF_4$:Yb/Nd@RB) triggered by a single 808 nm laser for dual modal UCL and MRI imaging-guided tumor PDT (Fig. 10) [124]. This imaging-guided treatment strategy could not only evaluate the dose and retention of therapeutics tumor deliver, but also achieved efficient inhibition of tumor growth and metastasis with minimized laser heating effect.

In another study, Lin et al. constructed $NaYF_4$:Yb/Er@$NaGdF_4$:Yb@$mSiO_2$-PEG@DOX based nanoplatforms that also provided the dual modality of UCL and MRI [177], meanwhile, such multifunctional UCNCs have been successfully applied for bioimaging and used as an anticancer drug delivery nanocarrier *in vitro* and *in vivo*.

5.4. UCL/MRI/CT-guided therapy

In addition to that UCNPs can act as MRI contrast agents, Yb-doped UCNPs have been applied for computed tomography (CT) bioimaging because of their high atomic and strong X-ray attenuation [178]. In this aspect, Lin et al. developed a multifunctional drug delivery system combining UCL/MRI/CT trimodality imaging and NIR-activated platinum prodrug delivery (Fig. 11), this study provided complete information to guide the cancer treatment [62]. Besides, Hu et al. introduced another type of tri-modal UCL/MRI/CT based upconversion nanoplatforms composed of UCNPs, CeOx, graphite-C_3N_4 (g-C_3N_4) NPs, and metformin (Met) for tumor imaging and combined phototherapy *in vitro* and *in vivo* [179].

6. Perspective and conclusion

Over the past decade, upconversion photocontrolled therapeutic studies have achieved remarkable success in the treatment of critical diseases. Such NIR phototherapy paradigms greatly promote the modern precision medicine in living systems, owing to its enhanced therapy efficacy, high spatiotemporal controllability, deep-tissue penetrability and minimal invasiveness. However, despite the significant achievements, there are still some questions remain in the upconversion-mediated phototherapeutics for future clinical translations.

For instance, (1) How to unify the technical standards of upconversion nanomedicine? Although the preparation of UCNPs-based therapeutic nanoplatforms, the practical photo-manipulation as well as the animal experimental operations have been reported with standardized protocols, it is still difficult to obtain the comparative results with satisfied reproducibility and robustness varying from different research groups. Moreover, the technical standards for practically enhancing the upconversion quantum yields need to be clearly formulated. (2) How to minimize the nanotoxicity of UCNCs? Extensive studies disclosed that the rational optimization of the chemical composition, size distribution and surface modifications could significantly improve the biocompatibility of UCNCs for biomedical applications, but there are lack of tests to evaluate the long term toxicity, such as the potential immune response and mutagenic effects; (3) How to bridge the technical gap for the clinical translation? To date, no UCNC-based phototherapeutics has been applied in human beings, it is mainly due to either the biosafety issues or the treatment effects. There is a long way to update the technical standards from experimental animals to the human level, such as the dose-effect relationship, pharmacokinetics, administration modes, laser treatment and monitoring protocols.

In summary, the multifunctional upconversion-mediated therapeutics photorelease provides great opportunities for realizing the precision medicine in practice. In line with the effective efforts to improve the efficacy, minimizing the toxicity and standardizing the protocols, we envision that the NIR phototherapy *via* UCNCs will be getting closer to clinical applications against life-threatening diseases.

Declaration of Competing Interest

The authors declare no conflict of interest.

Acknowledgements

B.X. acknowledges the financial supports from NTU-AIT-MUV NAM/16001, Tier 1 RG5/18 (S), SSIJRI (203-A018003), MOE 2017-T2-2-110, A*Star SERC A1983c0028 (M4070319), SPMS-M4082042.110 awarded in Nanyang Technological University (NTU), Singapore and National Natural Science Foundation of China (NSFC) (No. 51929201), China.

References

[1] T.A. Yap, C.P. Carden, S.B. Kaye, Beyond chemotherapy: targeted therapies in ovarian cancer, Nat. Rev. Cancer 9 (2009) 167.
[2] J.M. Llovet, A. Villanueva, A. Lachenmayer, R.S. Finn, Advances in targeted therapies for hepatocellular carcinoma in the genomic era, Nat. Rev. Clin. Oncol. 12 (2015) 408.
[3] B.W. Haak, M. Levi, W.J. Wiersinga, Microbiota-targeted therapies on the intensive care unit, Curr. Opin. Crit. Care 23 (2017) 167–174.
[4] C. Saraiva, C. Praça, R. Ferreira, T. Santos, L. Ferreira, L. Bernardino, Nanoparticle-mediated brain drug delivery: overcoming blood–brain barrier to treat neurodegenerative diseases, J. Control. Release 235 (2016) 34–47.
[5] M. Katsuno, F. Tanaka, G. Sobue, Perspectives on molecular targeted therapies and clinical trials for neurodegenerative diseases, J. Neurol. Neurosurg. Psychiatry 83 (2012) 329–335.
[6] Y. Qiao, J. Wan, L. Zhou, W. Ma, Y. Yang, W. Luo, Z. Yu, H. Wang, Stimuli-responsive nanotherapeutics for precision drug delivery and cancer therapy, Wiley Interdiscip. Rev. Nanomed. Nanobiotechnol. 11 (2019) e1527.
[7] M.W. Tibbitt, J.E. Dahlman, R. Langer, Emerging frontiers in drug delivery, J. Am. Chem. Soc. 138 (2016) 704–717.
[8] A. Chan, R.P. Orme, R.A. Fricker, P. Roach, Remote and local control of stimuli responsive materials for therapeutic applications, Adv. Drug Deliv. Rev. 65 (2013) 497–514.
[9] X. Wang, X. Wang, S. Jin, N. Muhammad, Z. Guo, Stimuli-responsive therapeutic metallodrugs, Chem. Rev. 119 (2018) 1138–1192.
[10] C. Delas Heras Alarcón, S. Pennadam, C. Alexander, Stimuli responsive polymers for biomedical applications, Chem. Soc. Rev. 34 (2005) 276–285.
[11] H. Hatakeyama, Recent advances in endogenous and exogenous stimuli-responsive nanocarriers for drug delivery and therapeutics, Chem. Pharm. Bull. (Tokyo) 65 (2017) 612–617.
[12] D. Rosenblum, N. Joshi, W. Tao, J.M. Karp, D. Peer, Progress and challenges towards targeted delivery of cancer therapeutics, Nat. Commun. 9 (2018) 1–12.
[13] J. Shi, P.W. Kantoff, R. Wooster, O.C. Farokhzad, Cancer nanomedicine: progress, challenges and opportunities, Nat. Rev. Cancer 17 (2017) 20.
[14] X. Ai, J. Mu, B. Xing, Recent advances of light-mediated theranostics, Theranostics 6 (2016) 2439.
[15] J.M. Silva, E. Silva, R.L. Reis, Light-triggered release of photocaged therapeutics-where are we now? J. Control. Release 298 (2019) 164–176.
[16] Y. Yang, J. Mu, B. Xing, Photoactivated drug delivery and bioimaging, Wiley Interdiscip. Rev. Nanomed. Nanobiotechnol. 9 (2017) e1408.
[17] A. Barhoumi, Q. Liu, D.S. Kohane, Ultraviolet light-mediated drug delivery: principles, applications, and challenges, J. Control. Release 219 (2015) 31–42.
[18] C.G. Dariva, J.F. Coelho, A.C. Serra, Near infrared light-triggered nanoparticles using singlet oxygen photocleavage for drug delivery systems, J. Control. Release 294 (2019) 337–354.
[19] Z. Zhang, J. Wang, C. Chen, Near-infrared light-mediated nanoplatforms for cancer thermo-chemotherapy and optical imaging, Adv. Mater. 25 (2013) 3869–3880.
[20] J. Olejniczak, C.-J. Carling, A. Almutairi, Photocontrolled release using one-photon absorption of visible or NIR light, J. Control. Release 219 (2015) 18–30.
[21] A. Bansal, Y. Zhang, Photocontrolled nanoparticle delivery systems for biomedical applications, Acc. Chem. Res. 47 (2014) 3052–3060.
[22] G. Jalani, V. Tam, F. Vetrone, M. Cerruti, Seeing, targeting and delivering with upconverting nanoparticles, J. Am. Chem. Soc. 140 (2018) 10923–10931.
[23] A. Bagheri, H. Arandiyan, C. Boyer, M. Lim, Lanthanide-doped upconversion nanoparticles: emerging intelligent light-activated drug delivery systems, Adv. Sci. 3

(2016) 1500437.
[24] G. Tian, X. Zhang, Z. Gu, Y. Zhao, Recent advances in upconversion nanoparticles-based multifunctional nanocomposites for combined cancer therapy, Adv. Mater. 27 (2015) 7692–7712.
[25] S. Wang, A. Bi, W. Zeng, Z. Cheng, Upconversion nanocomposites for photo-based cancer theranostics, J. Mater. Chem. B 4 (2016) 5331–5348.
[26] L. Liu, S. Wang, B. Zhao, P. Pei, Y. Fan, X. Li, F. Zhang, Er3+ sensitized 1530 nm to 1180 nm second near-infrared window upconversion nanocrystals for in vivo biosensing, Angew. Chem. Int. Ed. 57 (2018) 7518–7522.
[27] M. Zhao, B. Li, P. Wang, L. Lu, Z. Zhang, L. Liu, S. Wang, D. Li, R. Wang, F. Zhang, Supramolecularly engineered NIR-II and upconversion nanoparticles in vivo assembly and disassembly to improve bioimaging, Adv. Mater. 30 (2018) 1804982.
[28] M. Zhao, R. Wang, B. Li, Y. Fan, Y. Wu, X. Zhu, F. Zhang, Precise in vivo inflammation imaging using in situ responsive cross-linking of glutathione-modified ultra-small NIR-II lanthanide nanoparticles, Angew. Chem. 131 (2019) 2072–2076.
[29] X. Li, L. Zhou, Y. Wei, A.M. El-Toni, F. Zhang, D. Zhao, Anisotropic growth-induced synthesis of dual-compartment Janus mesoporous silica nanoparticles for bimodal triggered drugs delivery, J. Am. Chem. Soc. 136 (2014) 15086–15092.
[30] C. Yao, W. Wang, P. Wang, M. Zhao, X. Li, F. Zhang, Near-infrared upconversion mesoporous cerium oxide hollow biophotocatalyst for concurrent pH-/H2O2-responsive O2-evolving synergetic cancer therapy, Adv. Mater. 30 (2018) 1704833.
[31] M. Haase, H. Schäfer, Upconverting nanoparticles, Angew. Chem. Int. Ed. 50 (2011) 5808–5829.
[32] V. Muhr, S. Wilhelm, T. Hirsch, O.S. Wolfbeis, Upconversion nanoparticles: from hydrophobic to hydrophilic surfaces, Acc. Chem. Res. 47 (2014) 3481–3493.
[33] G. Chen, H. Qiu, P.N. Prasad, X. Chen, Upconversion nanoparticles: design, nanochemistry, and applications in theranostics, Chem. Rev. 114 (2014) 5161–5214.
[34] X. Chen, D. Peng, Q. Ju, F. Wang, Photon upconversion in core–shell nanoparticles, Chem. Soc. Rev. 44 (2015) 1318–1330.
[35] J. Shen, G. Chen, A.M. Vu, W. Fan, O.S. Bilsel, C.C. Chang, G. Han, Engineering the upconversion nanoparticle excitation wavelength: cascade sensitization of tri-doped upconversion colloidal nanoparticles at 800 nm, Adv. Opt. Mater. 1 (2013) 644–650.
[36] F. Wang, X. Liu, Upconversion multicolor fine-tuning: visible to near-infrared emission from lanthanide-doped NaYF4 nanoparticles, J. Am. Chem. Soc. 130 (2008) 5642–5643.
[37] S. Han, R. Deng, X. Xie, X. Liu, Enhancing luminescence in lanthanide-doped upconversion nanoparticles, Angew. Chem. Int. Ed. 53 (2014) 11702–11715.
[38] L. Lyu, H. Cheong, X. Ai, W. Zhang, J. Li, H. Yang, J. Lin, B. Xing, Near-infrared light-mediated rare-earth nanocrystals: recent advances in improving photon conversion and alleviating the thermal effect, NPG Asia Mater. 10 (2018) 685.
[39] Y. Wang, K. Zheng, S. Song, D. Fan, H. Zhang, X. Liu, Remote manipulation of upconversion luminescence, Chem. Soc. Rev. 47 (2018) 6473–6485.
[40] W. Feng, C. Han, F. Li, Upconversion-nanophosphor-based functional nanocomposites, Adv. Mater. 25 (2013) 5287–5303.
[41] W. Feng, X. Zhu, F. Li, Recent advances in the optimization and functionalization of upconversion nanomaterials for in vivo bioapplications, NPG Asia Mater. 5 (2013) e75.
[42] V. Ramamurthy, J. Sivaguru, Supramolecular photochemistry as a potential synthetic tool: photocycloaddition, Chem. Rev. 116 (2016) 9914–9993.
[43] S. Wu, H.-J. Butt, Near-infrared photochemistry at interfaces based on upconverting nanoparticles, Phys. Chem. Chem. Phys. 19 (2017) 23585–23596.
[44] A. Terenzi, L. Salassa, Near-infrared photochemistry assisted by upconverting nanoparticles, Photoactive Inorganic Nanoparticles, Elsevier, 2019, pp. 43–71.
[45] C.J. Carling, F. Nourmohammadian, J.C. Boyer, N.R. Branda, Remote-control photorelease of caged compounds using near-infrared light and upconverting nanoparticles, Angew. Chem. Int. Ed. 49 (2010) 3782–3785.
[46] B. Yan, J.-C. Boyer, N.R. Branda, Y. Zhao, Near-infrared light-triggered dissociation of block copolymer micelles using upconverting nanoparticles, J. Am. Chem. Soc. 133 (2011) 19714–19717.
[47] B. Yan, J.-C. Boyer, D. Habault, N.R. Branda, Y. Zhao, Near infrared light triggered release of biomacromolecules from hydrogels loaded with upconversion nanoparticles, J. Am. Chem. Soc. 134 (2012) 16558–16561.
[48] G. Jalani, R. Naccache, D.H. Rosenzweig, L. Haglund, F. Vetrone, M. Cerruti, Photocleavable hydrogel-coated upconverting nanoparticles: a multifunctional theranostic platform for NIR imaging and on-demand macromolecular delivery, J. Am. Chem. Soc. 138 (2016) 1078–1083.
[49] M.L. Viger, M. Grossman, N. Fomina, A. Almutairi, Low power upconverted near-ir light for efficient polymeric nanoparticle degradation and cargo release, Adv. Mater. 25 (2013) 3733–3738.
[50] Y.-C. Chung, C.-H. Yang, R.-H. Lee, T.-L. Wang, Dual stimuli-responsive block copolymers for controlled release triggered by upconversion luminescence or temperature variation, ACS Omega 4 (2019) 3322–3328.
[51] Y. Yang, Q. Shao, R. Deng, C. Wang, X. Teng, K. Cheng, Z. Cheng, L. Huang, Z. Liu, X. Liu, In vitro and in vivo uncaging and bioluminescence imaging by using photocaged upconversion nanoparticles, Angew. Chem. Int. Ed. 51 (2012) 3125–3129.
[52] Y. Yang, B. Velmurugan, X. Liu, B. Xing, NIR photoresponsive crosslinked upconverting nanocarriers toward selective intracellular drug release, Small 9 (2013) 2937–2944.
[53] P.T. Wong, D. Chen, S. Tang, S. Yanik, M. Payne, J. Mukherjee, A. Coulter, K. Tang, K. Tao, K. Sun, Modular integration of upconverting nanocrystal–dendrimer composites for folate receptor-specific NIR imaging and light-triggered drug release, Small 11 (2015) 6078–6090.
[54] M.K.G. Jayakumar, N.M. Idris, Y. Zhang, Remote activation of biomolecules in deep tissues using near-infrared-to-UV upconversion nanotransducers, Proc. Natl. Acad. Sci. 109 (2012) 8483–8488.
[55] Y. Yang, F. Liu, X. Liu, B. Xing, NIR light controlled photorelease of siRNA and its targeted intracellular delivery based on upconversion nanoparticles, Nanoscale 5 (2013) 231–238.
[56] Y.-H. Chien, Y.-L. Chou, S.-W. Wang, S.-T. Hung, M.-C. Liau, Y.-J. Chao, C.-H. Su, C.-S. Yeh, Near-infrared light photocontrolled targeting, bioimaging, and chemotherapy with caged upconversion nanoparticles in vitro and in vivo, ACS Nano 7 (2013) 8516–8528.
[57] H.-D. Gao, P. Thanasekaran, C.-W. Chiang, J.-L. Hong, Y.-C. Liu, Y.-H. Chang, H.-M. Lee, Construction of a near-infrared-activatable enzyme platform to remotely trigger intracellular signal transduction using an upconversion nanoparticle, ACS Nano 9 (2015) 7041–7051.
[58] L.L. Fedoryshin, A.J. Tavares, E. Petryayeva, S. Doughan, U.J. Krull, Near-infrared-triggered anticancer drug release from upconverting nanoparticles, ACS Appl. Mater. Interfaces 6 (2014) 13600–13606.
[59] J. Shen, G. Chen, T.Y. Ohulchanskyy, S.J. Kesseli, S. Buchholz, Z. Li, P.N. Prasad, G. Han, Tunable near infrared to ultraviolet upconversion luminescence enhancement in (α-NaYF4: Yb, Tm)/CaF2 core/shell nanoparticles for in situ real-time recorded biocompatible photoactivation, Small 9 (2013) 3213–3217.
[60] L. Zhao, J. Peng, Q. Huang, C. Li, M. Chen, Y. Sun, Q. Lin, L. Zhu, F. Li, Near-infrared photoregulated drug release in living tumor tissue via yolk-shell upconversion nanocages, Adv. Funct. Mater. 24 (2014) 363–371.
[61] Y. Min, J. Li, F. Liu, E.K. Yeow, B. Xing, Near-infrared light-mediated photoactivation of a platinum antitumor prodrug and simultaneous cellular apoptosis imaging by upconversion-luminescent nanoparticles, Angew. Chem. Int. Ed. 53 (2014) 1012–1016.
[62] Y. Dai, H. Xiao, J. Liu, Q. Yuan, P.A. Ma, D. Yang, C. Li, Z. Cheng, Z. Hou, P. Yang, In vivo multimodality imaging and cancer therapy by near-infrared light-triggered trans-platinum pro-drug-conjugated upconverison nanoparticles, J. Am. Chem. Soc. 135 (2013) 18920–18929.
[63] P.A. Ma, H. Xiao, X. Li, C. Li, Y. Dai, Z. Cheng, X. Jing, J. Lin, Rational design of multifunctional upconversion nanocrystals/polymer nanocomposites for cisplatin (IV) delivery and biomedical imaging, Adv. Mater. 25 (2013) 4898–4905.
[64] E. Ruggiero, J. Hernández-Gil, J.C. Mareque-Rivas, L. Salassa, Near infrared activation of an anticancer PtIV complex by Tm-doped upconversion nanoparticles, Chem. Commun. 51 (2015) 2091–2094.
[65] S. Perfahl, M.M. Natile, H.S. Mohamad, C.A. Helm, C. Schulzke, G. Natile, P.J. Bednarski, Photoactivation of diiodido–Pt (IV) complexes coupled to upconverting nanoparticles, Mol. Pharm. 13 (2016) 2346–2362.
[66] Y. Dai, H. Bi, X. Deng, C. Li, F. He, P. Yang, J. Lin, 808 nm near-infrared light controlled dual-drug release and cancer therapy in vivo by upconversion mesoporous silica nanostructures, J. Mater. Chem. B 5 (2017) 2086–2095.
[67] J. Xu, Y. Kuang, R. Lv, P. Yang, C. Li, H. Bi, B. Liu, D. Yang, Y. Dai, S. Gai, Charge convertibility and near infrared photon co-enhanced cisplatin chemotherapy based on upconversion nanoplatform, Biomaterials 130 (2017) 42–55.
[68] S. He, K. Krippes, S. Ritz, Z. Chen, A. Best, H.-J. Butt, V. Mailänder, S. Wu, Ultralow-intensity near-infrared light induces drug delivery by upconverting nanoparticles, Chem. Commun. 51 (2015) 431–434.
[69] Y. Zhang, Z. Yu, J. Li, Y. Ao, J. Xue, Z. Zeng, X. Yang, T.T.Y. Tan, Ultrasmall-superbright neodymium-upconversion nanoparticles via energy migration manipulation and lattice modification: 808 nm-activated drug release, ACS Nano 11 (2017) 2846–2857.
[70] H. Wang, R.-l. Han, L.-m. Yang, J.-h. Shi, Z.-j. Liu, Y. Hu, Y. Wang, S.-j. Liu, Y. Gan, Design and synthesis of core–shell–shell upconversion nanoparticles for NIR-induced drug release, photodynamic therapy, and cell imaging, ACS Appl. Mater. Interfaces 8 (2016) 4416–4423.
[71] Z. Liu, J. Shi, Y. Wang, Y. Gan, P. Wan, Facile preparation of pyrenemethyl ester-based nanovalve on mesoporous silica coated upconversion nanoparticle for NIR light-triggered drug release with potential monitoring capability, Colloids Surf. A Physicochem. Eng. Asp. 568 (2019) 436–444.
[72] J.V. Garcia, J. Yang, D. Shen, C. Yao, X. Li, R. Wang, G.D. Stucky, D. Zhao, P.C. Ford, F. Zhang, NIR-triggered release of caged nitric oxide using upconverting nanostructured materials, Small 8 (2012) 3800–3805.
[73] P.T. Burks, J.V. Garcia, R. GonzalezIrias, J.T. Tillman, M. Niu, A.A. Mikhailovsky, J. Zhang, F. Zhang, P.C. Ford, Nitric oxide releasing materials triggered by near-infrared excitation through tissue filters, J. Am. Chem. Soc. 135 (2013) 18145–18152.
[74] X. Zhang, G. Tian, W. Yin, L. Wang, X. Zheng, L. Yan, J. Li, H. Su, C. Chen, Z. Gu, Controllable generation of nitric oxide by near-infrared-sensitized upconversion nanoparticles for tumor therapy, Adv. Funct. Mater. 25 (2015) 3049–3056.
[75] X. Zhang, Z. Guo, J. Liu, G. Tian, K. Chen, S. Yu, Z. Gu, Near infrared light triggered nitric oxide releasing platform based on upconversion nanoparticles for synergistic therapy of cancer stem-like cells, Sci. Bull. 62 (2017) 985–996.
[76] A.E. Pierri, P.-J. Huang, J.V. Garcia, J.G. Stanfill, M. Chui, G. Wu, N. Zheng, P.C. Ford, A photoCORM nanocarrier for CO release using NIR light, Chem. Commun. 51 (2015) 2072–2075.
[77] J. Ou, W. Zheng, Z. Xiao, Y. Yan, X. Jiang, Y. Dou, R. Jiang, X. Liu, Core–shell materials bearing iron (ii) carbonyl units and their CO-release via an upconversion process, J. Mater. Chem. B 5 (2017) 8161–8168.
[78] W. Chen, M. Chen, Q. Zang, L. Wang, F. Tang, Y. Han, C. Yang, L. Deng, Y.-N. Liu, NIR light controlled release of caged hydrogen sulfide based on upconversion nanoparticles, Chem. Commun. 51 (2015) 9193–9196.
[79] T. Wu, M. Barker, K.M. Arafeh, J.C. Boyer, C.J. Carling, N.R. Branda, A UV-blocking polymer shell prevents one-photon photoreactions while allowing multi-photon processes in encapsulated upconverting nanoparticles, Angew. Chem. Int.

Ed. 52 (2013) 11106–11109.
[80] J. Liu, W. Bu, L. Pan, J. Shi, NIR-triggered anticancer drug delivery by upconverting nanoparticles with integrated azobenzene-modified mesoporous silica, Angew. Chem. Int. Ed. 52 (2013) 4375–4379.
[81] C. Yao, P. Wang, X. Li, X. Hu, J. Hou, L. Wang, F. Zhang, Near-infrared-triggered azobenzene-liposome/upconversion nanoparticle hybrid vesicles for remotely controlled drug delivery to overcome cancer multidrug resistance, Adv. Mater. 28 (2016) 9341–9348.
[82] G. Chen, B. Ma, R. Xie, Y. Wang, K. Dou, S. Gong, NIR-induced spatiotemporally controlled gene silencing by upconversion nanoparticle-based siRNA nanocarrier, J. Control. Release 282 (2018) 148–155.
[83] S. Chen, Y. Gao, Z. Cao, B. Wu, L. Wang, H. Wang, Z. Dang, G. Wang, Nanocomposites of spiropyran-functionalized polymers and upconversion nanoparticles for controlled release stimulated by near-infrared light and pH, Macromolecules 49 (2016) 7490–7496.
[84] L. Zhou, Z. Chen, K. Dong, M. Yin, J. Ren, X. Qu, DNA-mediated construction of hollow upconversion nanoparticles for protein harvesting and near-infrared light triggered release, Adv. Mater. 26 (2014) 2424–2430.
[85] L. He, Y. Zhang, G. Ma, P. Tan, Z. Li, S. Zang, X. Wu, J. Jing, S. Fang, L. Zhou, Near-infrared photoactivatable control of Ca2+ signaling and optogenetic immunomodulation, Elife 4 (2015) e10024.
[86] S. Shah, J.-J. Liu, N. Pasquale, J. Lai, H. McGowan, Z.P. Pang, K.-B. Lee, Hybrid upconversion nanomaterials for optogenetic neuronal control, Nanoscale 7 (2015) 16571–16577.
[87] A. Bansal, H. Liu, M.K.G. Jayakumar, S. Andersson-Engels, Y. Zhang, Quasi-continuous wave near-infrared excitation of upconversion nanoparticles for optogenetic manipulation of C. elegans, Small 12 (2016) 1732–1743.
[88] A. Pliss, T.Y. Ohulchanskyy, G. Chen, J. Damasco, C.E. Bass, P.N. Prasad, Subcellular optogenetics enacted by targeted nanotransformers of near-infrared light, ACS Photon. 4 (2017) 806–814.
[89] K. Yadav, A.-C. Chou, R.K. Ulaganathan, H.-D. Gao, H.-M. Lee, C.-Y. Pan, Y.-T. Chen, Targeted and efficient activation of channelrhodopsins expressed in living cells via specifically-bound upconversion nanoparticles, Nanoscale 9 (2017) 9457–9466.
[90] Y. Wang, K. Xie, H. Yue, X. Chen, X. Luo, Q. Liao, M. Liu, F. Wang, P. Shi, Flexible and fully implantable upconversion device for wireless optogenetic stimulation of the spinal cord in behaving animals, Nanoscale 12 (2020) 2406–2414.
[91] X. Ai, L. Lyu, Y. Zhang, Y. Tang, J. Mu, F. Liu, Y. Zhou, Z. Zuo, G. Liu, B. Xing, Remote regulation of membrane channel activity by site-specific localization of lanthanide-doped upconversion nanocrystals, Angew. Chem. Int. Ed. 56 (2017) 3031–3035.
[92] S. Hososhima, H. Yuasa, T. Ishizuka, M.R. Hoque, T. Yamashita, A. Yamanaka, E. Sugano, H. Tomita, H. Yawo, Near-infrared (NIR) up-conversion optogenetics, Sci. Rep. 5 (2015) 16533.
[93] X. Lin, Y. Wang, X. Chen, R. Yang, Z. Wang, J. Feng, H. Wang, K.W. Lai, J. He, F. Wang, Multiplexed optogenetic stimulation of neurons with spectrum-selective upconversion nanoparticles, Adv. Healthc. Mater. 6 (2017) 1700446.
[94] Y. Wang, X. Lin, X. Chen, X. Chen, Z. Xu, W. Zhang, Q. Liao, X. Duan, X. Wang, M. Liu, Tetherless near-infrared control of brain activity in behaving animals using fully implantable upconversion microdevices, Biomaterials 142 (2017) 136–148.
[95] X. Wu, Y. Zhang, K. Takle, O. Bilsel, Z. Li, H. Lee, Z. Zhang, D. Li, W. Fan, C. Duan, Dye-sensitized core/active shell upconversion nanoparticles for optogenetics and bioimaging applications, ACS Nano 10 (2016) 1060–1066.
[96] X. Lin, X. Chen, W. Zhang, T. Sun, P. Fang, Q. Liao, X. Chen, J. He, M. Liu, F. Wang, Core–shell–shell upconversion nanoparticles with enhanced emission for wireless optogenetic inhibition, Nano Lett. 18 (2018) 948–956.
[97] S. Chen, A.Z. Weitemier, X. Zeng, L. He, X. Wang, Y. Tao, A.J. Huang, Y. Hashimotodani, M. Kano, H. Iwasaki, Near-infrared deep brain stimulation via upconversion nanoparticle–mediated optogenetics, Science 359 (2018) 679–684.
[98] Y. Ao, K. Zeng, B. Yu, Y. Miao, W. Hung, Z. Yu, Y. Xue, T.T.Y. Tan, T. Xu, M. Zhen, An upconversion nanoparticle enables near infrared-optogenetic manipulation of the caenorhabditis elegans motor circuit, ACS Nano 13 (2019) 3373–3386.
[99] Q. Mei, A. Bansal, M.K.G. Jayakumar, Z. Zhang, J. Zhang, H. Huang, D. Yu, C.J. Ramachandra, D.J. Hausenloy, T.W. Soong, Manipulating energy migration within single lanthanide activator for switchable upconversion emissions towards bidirectional photoactivation, Nat. Commun. 10 (2019) 1–11.
[100] B. Zheng, H. Wang, H. Pan, C. Liang, W. Ji, L. Zhao, H. Chen, X. Gong, X. Wu, J. Chang, Near-infrared light triggered upconversion optogenetic nanosystem for cancer therapy, ACS Nano 11 (2017) 11898–11907.
[101] H.S. Qian, H.C. Guo, P.C.L. Ho, R. Mahendran, Y. Zhang, Mesoporous-Silica-coated up-conversion fluorescent nanoparticles for photodynamic therapy, Small 5 (2009) 2285–2290.
[102] N.M. Idris, M.K. Gnanasammandhan, J. Zhang, P.C. Ho, R. Mahendran, Y. Zhang, In vivo photodynamic therapy using upconversion nanoparticles as remote-controlled nanotransducers, Nat. Med. 18 (2012) 1580–1585.
[103] L. Xia, X. Kong, X. Liu, L. Tu, Y. Zhang, Y. Chang, K. Liu, D. Shen, H. Zhao, H. Zhang, An upconversion nanoparticle–zinc phthalocyanine based nanophotosensitizer for photodynamic therapy, Biomaterials 35 (2014) 4146–4156.
[104] J. Xu, D. Yang, R. Lv, B. Liu, S. Gai, F. He, C. Li, P. Yang, Design, fabrication, luminescence and biomedical applications of UCNPs@mSiO2–ZnPc–CDs–P (NIPAm-MAA) nanocomposites, J. Mater. Chem. B 4 (2016) 5883–5894.
[105] X. Jia, H.N. Ye, H. Weng, N. Huang, Y. Yu, J.P. Xue, Small molecular target-based multifunctional upconversion nanocomposites for targeted and in-depth photodynamic and chemo-anticancer therapy, Mater. Sci. Eng. C Mater. Biol. Appl. 104 (2019) 109849.
[106] Y. Liu, Y. Liu, W. Bu, C. Cheng, C. Zuo, Q. Xiao, Y. Sun, D. Ni, C. Zhang, J. Liu, Hypoxia induced by upconversion-based photodynamic therapy: towards highly effective synergistic bioreductive therapy in tumors, Angew. Chem. Int. Ed. 54 (2015) 8105–8109.
[107] J. Xu, D. Yang, R. Lv, B. Liu, S. Gai, F. He, C. Li, P. Yang, Design, fabrication, luminescence and biomedical applications of UCNPs@ mSiO 2–ZnPc–CDs–P (NIPAm-MAA) nanocomposites, J. Mater. Chem. B 4 (2016) 5883–5894.
[108] Z. Zhang, M.K.G. Jayakumar, X. Zheng, S. Shikha, Y. Zhang, A. Bansal, D.J. Poon, P.L. Chu, E.L. Yeo, M.L. Chua, Upconversion superballs for programmable photoactivation of therapeutics, Nat. Commun. 10 (2019) 1–12.
[109] M. Tang, X. Zhu, Y. Zhang, Z. Zhang, Z. Zhang, Q. Mei, J. Zhang, M. Wu, J. Liu, Y. Zhang, Near-infrared excited orthogonal emissive upconversion nanoparticles for imaging-guided on-demand therapy, ACS Nano 13 (2019) 10405–10418.
[110] Y.I. Park, H.M. Kim, J.H. Kim, K.C. Moon, B. Yoo, K.T. Lee, N. Lee, Y. Choi, W. Park, D. Ling, K. Na, W.K. Moon, S.H. Choi, H.S. Park, S.Y. Yoon, Y.D. Suh, S.H. Lee, T. Hyeon, Theranostic probe based on lanthanide-doped nanoparticles for simultaneous in vivo dual-modal imaging and photodynamic therapy, Adv. Mater. 24 (2012) 5755–5761.
[111] C. Wang, L. Cheng, Y. Liu, X. Wang, X. Ma, Z. Deng, Y. Li, Z. Liu, Imaging-guided pH-sensitive photodynamic therapy using charge reversible upconversion nanoparticles under near-infrared light, Adv. Funct. Mater. 23 (2013) 3077–3086.
[112] X. Wang, K. Liu, G. Yang, L. Cheng, L. He, Y. Liu, Y. Li, L. Guo, Z. Liu, Near-infrared light triggered photodynamic therapy in combination with gene therapy using upconversion nanoparticles for effective cancer cell killing, Nanoscale 6 (2014) 9198–9205.
[113] C. Wang, H. Tao, L. Cheng, Z. Liu, Near-infrared light induced in vivo photodynamic therapy of cancer based on upconversion nanoparticles, Biomaterials 32 (2011) 6145–6154.
[114] T. Zhang, H. Lin, L. Cui, N. An, R. Tong, Y. Chen, C. Yang, X. Li, J. Liu, F. Qu, Near infrared light triggered reactive oxygen species responsive upconversion nanoplatform for drug delivery and photodynamic therapy, Eur. J. Inorg. Chem. 2016 (2016) 1206–1213.
[115] J. Xu, L. Xu, C. Wang, R. Yang, Q. Zhuang, X. Han, Z. Dong, W. Zhu, R. Peng, Z. Liu, Near-infrared-triggered photodynamic therapy with multitasking upconversion nanoparticles in combination with checkpoint blockade for immunotherapy of colorectal cancer, ACS Nano 11 (2017) 4463–4474.
[116] X. Ai, C.J.H. Ho, J. Aw, A.B.E. Attia, J. Mu, Y. Wang, X. Wang, Y. Wang, X. Liu, H. Chen, In vivo covalent cross-linking of photon-converted rare-earth nanostructures for tumour localization and theranostics, Nat. Commun. 7 (2016) 10432.
[117] T. Gu, L. Cheng, F. Gong, J. Xu, X. Li, G. Han, Z. Liu, Upconversion composite nanoparticles for tumor hypoxia modulation and enhanced near-infrared-triggered photodynamic therapy, ACS Appl. Mater. Interfaces 10 (2018) 15494–15503.
[118] M. Guan, H. Dong, J. Ge, D. Chen, L. Sun, S. Li, C. Wang, C. Yan, P. Wang, C. Shu, Multifunctional upconversion–nanoparticles–trismethylpyridylporphyrin–fullerene nanocomposite: a near-infrared light-triggered theranostic platform for imaging-guided photodynamic therapy, NPG Asia Mater. 7 (2015) e205.
[119] L. He, M. Brasino, C. Mao, S. Cho, W. Park, A.P. Goodwin, J.N. Cha, DNA-assembled core-satellite upconverting-metal-organic framework nanoparticle superstructures for efficient photodynamic therapy, Small 13 (2017).
[120] Y. Li, Z. Di, J. Gao, P. Cheng, C. Di, G. Zhang, B. Liu, X. Shi, L.-D. Sun, L. Li, Heterodimers made of upconversion nanoparticles and metal–organic frameworks, J. Am. Chem. Soc. 139 (2017) 13804–13810.
[121] C. Liu, B. Liu, J. Zhao, Z. Di, D. Chen, Z. Gu, L. Li, Y. Zhao, Nd(3+) -sensitized upconversion metal-organic frameworks for mitochondria-targeted amplified photodynamic therapy, Angew. Chem. Int. Ed. (2019) 1–6.
[122] K. Liu, X. Liu, Q. Zeng, Y. Zhang, L. Tu, T. Liu, X. Kong, Y. Wang, F. Cao, S.A.G. Lambrechts, M.C.G. Aalders, H. Zhang, Covalently assembled NIR nanoplatform for simultaneous fluorescence imaging and photodynamic therapy of cancer cells, ACS Nano 6 (2012) 4054–4062.
[123] S. Wang, L. Zhang, C. Dong, L. Su, H. Wang, J. Chang, Smart pH-responsive upconversion nanoparticles for enhanced tumor cellular internalization and near-infrared light-triggered photodynamic therapy, Chem. Commun. 51 (2015) 406–408.
[124] Y. Li, J. Tang, D.X. Pan, L.D. Sun, C. Chen, Y. Liu, Y.F. Wang, S. Shi, C.H. Yan, A versatile imaging and therapeutic platform based on dual-band luminescent lanthanide nanoparticles toward tumor metastasis inhibition, ACS Nano 10 (2016) 2766–2773.
[125] D. Wang, B. Xue, X. Kong, L. Tu, X. Liu, Y. Zhang, Y. Chang, Y. Luo, H. Zhao, H. Zhang, 808 nm driven Nd 3+-sensitized upconversion nanostructures for photodynamic therapy and simultaneous fluorescence imaging, Nanoscale 7 (2015) 190–197.
[126] F. Ai, T. Sun, Z. Xu, Z. Wang, W. Kong, M.W. To, F. Wang, G. Zhu, An upconversion nanoplatform for simultaneous photodynamic therapy and Pt chemotherapy to combat cisplatin resistance, Dalton Trans. 45 (2016) 13052–13060.
[127] F. Lu, L. Yang, Y. Ding, J.-J. Zhu, Highly emissive Nd3+-sensitized multilayered upconversion nanoparticles for efficient 795 nm operated photodynamic therapy, Adv. Funct. Mater. 26 (2016) 4778–4785.
[128] G. Chen, R. Jaskula-Sztul, C.R. Esquibel, I. Lou, Q. Zheng, A. Dammalapati, A. Harrison, K.W. Eliceiri, W. Tang, H. Chen, Neuroendocrine tumor-targeted upconversion nanoparticle-based micelles for simultaneous NIR-controlled combination chemotherapy and photodynamic therapy, and fluorescence imaging, Adv. Funct. Mater. 27 (2017) 1604671.
[129] T. Sabri, P.D. Pawelek, J.A. Capobianco, Dual activity of Rose Bengal functionalized to albumin-coated lanthanide-doped upconverting nanoparticles: targeting and photodynamic therapy, ACS Appl. Mater. Interfaces 10 (2018) 26947–26953.
[130] S. Kuk, B.I. Lee, J.S. Lee, C.B. Park, Rattle-structured upconversion nanoparticles for near-IR-induced suppression of Alzheimer's β-amyloid aggregation, Small 13

(2017) 1603139.
[131] Z. Hou, Y. Zhang, K. Deng, Y. Chen, X. Li, X. Deng, Z. Cheng, H. Lian, C. Li, J. Lin, UV-emitting upconversion-based TiO2 photosensitizing nanoplatform: near-infrared light mediated in vivo photodynamic therapy via mitochondria-involved apoptosis pathway, ACS Nano 9 (2015) 2584–2599.
[132] S.S. Lucky, N. Muhammad Idris, Z. Li, K. Huang, K.C. Soo, Y. Zhang, Titania coated upconversion nanoparticles for near-infrared light triggered photodynamic therapy, ACS Nano 9 (2015) 191–205.
[133] S.S. Lucky, N.M. Idris, K. Huang, J. Kim, Z. Li, P.S.P. Thong, R. Xu, K.C. Soo, Y. Zhang, In vivo biocompatibility, biodistribution and therapeutic efficiency of titania coated upconversion nanoparticles for photodynamic therapy of solid oral cancers, Theranostics 6 (2016) 1844.
[134] M. Yin, E. Ju, Z. Chen, Z. Li, J. Ren, X. Qu, Upconverting nanoparticles with a mesoporous TiO2 shell for near-infrared-triggered drug delivery and synergistic targeted cancer therapy, Chem. Eur. J. 20 (2014) 14012–14017.
[135] Z. Hou, K. Deng, M. Wang, Y. Liu, M. Chang, S. Huang, C. Li, Y. Wei, Z. Cheng, G. Han, Hydrogenated titanium oxide decorated upconversion nanoparticles: facile laser modified synthesis and 808 nm near-infrared light triggered phototherapy, Chem. Mater. 31 (2019) 774–784.
[136] G. Yang, D. Yang, P. Yang, R. Lv, C. Li, C. Zhong, F. He, S. Gai, J. Lin, A single 808 nm near-infrared light-mediated multiple imaging and photodynamic therapy based on titania coupled upconversion nanoparticles, Chem. Mater. 27 (2015) 7957–7968.
[137] Z. Hou, K. Deng, C. Li, X. Deng, H. Lian, Z. Cheng, D. Jin, J. Lin, 808 nm Light-triggered and hyaluronic acid-targeted dual-photosensitizers nanoplatform by fully utilizing Nd(3+)-sensitized upconversion emission with enhanced anti-tumor efficacy, Biomaterials 101 (2016) 32–46.
[138] T. Jia, J. Xu, S. Dong, F. He, C. Zhong, G. Yang, H. Bi, M. Xu, Y. Hu, D. Yang, Mesoporous cerium oxide-coated upconversion nanoparticles for tumor-responsive chemo-photodynamic therapy and bioimaging, Chem. Sci. 10 (2019) 8618–8633.
[139] W. Jiang, C. Zhang, A. Ahmed, Y. Zhao, Y. Deng, Y. Ding, J. Cai, Y. Hu, H2O2-sensitive upconversion nanocluster bomb for tri-mode imaging-guided photodynamic therapy in deep tumor tissue, Adv. Healthc. Mater. 8 (2019) 1900972.
[140] Y. Yuan, Y. Min, Q. Hu, B. Xing, B. Liu, NIR photoregulated chemo-and photodynamic cancer therapy based on conjugated polyelectrolyte–drug conjugate encapsulated upconversion nanoparticles, Nanoscale 6 (2014) 11259–11272.
[141] H. Zhao, W. Hu, H. Ma, R. Jiang, Y. Tang, Y. Ji, X. Lu, B. Hou, W. Deng, W. Huang, Photo-induced charge-variable conjugated polyelectrolyte brushes encapsulating upconversion nanoparticles for promoted siRNA release and collaborative photodynamic therapy under NIR light irradiation, Adv. Funct. Mater. 27 (2017) 1702592.
[142] M. Hu, J. Zhao, X. Ai, M. Budanovic, J. Mu, R.D. Webster, Q. Cao, Z. Mao, B. Xing, Near infrared light-mediated photoactivation of cytotoxic Re(i) complexes by using lanthanide-doped upconversion nanoparticles, Dalton Trans. 45 (2016) 14101–14108.
[143] E.V. Khaydukov, K.E. Mironova, V.A. Semchishen, A.N. Generalova, A.V. Nechaev, D.A. Khochenkov, E.V. Stepanova, O.I. Lebedev, A.V. Zvyagin, S.M. Deyev, V.Y. Panchenko, Riboflavin photoactivation by upconversion nanoparticles for cancer treatment, Sci. Rep. 6 (2016) 35103.
[144] B. Ding, S. Shao, C. Yu, B. Teng, M. Wang, Z. Cheng, K.L. Wong, P.A. Ma, J. Lin, Large-pore mesoporous-silica-coated upconversion nanoparticles as multifunctional immunoadjuvants with ultrahigh photosensitizer and antigen loading efficiency for improved cancer photodynamic immunotherapy, Adv. Mater. 30 (2018) 1802479.
[145] L. Liang, Y. Lu, R. Zhang, A. Care, T.A. Ortega, S.M. Deyev, Y. Qian, A.V. Zvyagin, Deep-penetrating photodynamic therapy with KillerRed mediated by upconversion nanoparticles, Acta Biomater. 51 (2017) 461–470.
[146] G. Lee, Y.I. Park, Lanthanide-doped upconversion nanocarriers for drug and gene delivery, Nanomaterials 8 (2018) 511.
[147] J. Zhao, J. Gao, W. Xue, Z. Di, H. Xing, Y. Lu, L. Li, Upconversion luminescence-activated DNA nanodevice for ATP sensing in living cells, J. Am. Chem. Soc. 140 (2018) 578–581.
[148] J. Zhao, H. Chu, Y. Zhao, Y. Lu, L. Li, A NIR light gated DNA nanodevice for spatiotemporally controlled imaging of MicroRNA in cells and animals, J. Am. Chem. Soc. 141 (2019) 7056–7062.
[149] D. Scaini, L. Ballerini, Nanomaterials at the neural interface, Curr. Opin. Neurobiol. 50 (2018) 50–55.
[150] P. Tan, L. He, G. Han, Y. Zhou, Optogenetic immunomodulation: shedding light on antitumor immunity, Trends Biotechnol. 35 (2017) 215–226.
[151] M. Endo, T. Ozawa, Strategies for development of optogenetic systems and their applications, J Photochem Photobiol C: Photochem Rev 30 (2017) 10–23.
[152] Z. Wang, M. Hu, X. Ai, Z. Zhang, B. Xing, Near-infrared manipulation of membrane ion channels via upconversion optogenetics, Adv. Biosys. 3 (2019) 1800233.
[153] A.H. All, X. Zeng, D.B.L. Teh, Z. Yi, A. Prasad, T. Ishizuka, N. Thakor, Y. Hiromu, X. Liu, Expanding the Toolbox of upconversion nanoparticles for in vivo optogenetics and neuromodulation, Adv. Mater. 31 (2019) 1803474.
[154] N. Yu, L. Huang, Y. Zhou, T. Xue, Z. Chen, G. Han, Near-infrared-light activatable nanoparticles for deep-tissue-penetrating wireless optogenetics, Adv. Healthc. Mater. 8 (2019) 1801132.
[155] P. Agostinis, K. Berg, K.A. Cengel, T.H. Foster, A.W. Girotti, S.O. Gollnick, S.M. Hahn, M.R. Hamblin, A. Juzeniene, D. Kessel, M. Korbelik, J. Moan, P. Mroz, D. Nowis, J. Piette, B.C. Wilson, J. Golab, Photodynamic therapy of cancer: an update, CA Cancer J. Clin. 61 (2011) 250–281.
[156] X. Zhao, Y. Huang, G. Yuan, K. Zuo, Y. Huang, J.-J. Chen, J. Li, J. Xue, A novel tumor and mitochondria dual-targeted photosensitizer showing ultra-efficient photodynamic anticancer activities, Chem. Commun. 55 (2018) 866–869.
[157] J. Zhu, C. Chu, D. Li, X. Pang, H. Zheng, J. Wang, Y. Shi, Y. Zhang, Y. Cheng, E. Ren, J. Cheng, X. Chen, G. Liu, Fe(III)-porphyrin sonotheranostics: a green triple-regulated ROS generation nanoplatform for enhanced cancer imaging and therapy, Adv. Funct. Mater. 29 (2019).
[158] W. Fan, P. Huang, X. Chen, Overcoming the Achilles' heel of photodynamic therapy, Chem. Soc. Rev. 45 (2016) 6488–6519.
[159] C. Wang, L. Cheng, Z. Liu, Upconversion nanoparticles for photodynamic therapy and other cancer therapeutics, Theranostics 3 (2013) 317.
[160] T. Pirmohamed, J.M. Dowding, S. Singh, B. Wasserman, E. Heckert, A.S. Karakoti, J.E. King, S. Seal, W.T. Self, Nanoceria exhibit redox state-dependent catalase mimetic activity, Chem. Commun. 46 (2010) 2736–2738.
[161] E.L. Cates, M. Cho, J.-H. Kim, Converting visible light into UVC: microbial inactivation by Pr3+-activated upconversion materials, Environ. Sci. Technol. 45 (2011) 3680–3686.
[162] S.L. Cates, E.L. Cates, M. Cho, J.-H. Kim, Synthesis and characterization of visible-to-UVC upconversion antimicrobial ceramics, Environ. Sci. Technol. 48 (2014) 2290–2297.
[163] F. Xu, M. Hu, C. Liu, S.K. Choi, Yolk-structured multifunctional up-conversion nanoparticles for synergistic photodynamic–sonodynamic antibacterial resistance therapy, Biomater. Sci. 5 (2017) 678–685.
[164] Y. Zhang, P. Huang, D. Wang, J. Chen, W. Liu, P. Hu, M. Huang, X. Chen, Z. Chen, Near-infrared-triggered antibacterial and antifungal photodynamic therapy based on lanthanide-doped upconversion nanoparticles, Nanoscale 10 (2018) 15485–15495.
[165] M.C. Grüner, M.S. Arai, M. Carreira, N. Inada, A.S. de Camargo, Functionalizing the mesoporous silica shell of upconversion nanoparticles to enhance bacterial targeting and killing via photosensitizer-induced antimicrobial photodynamic therapy, ACS Appl. Bio. Mater. 1 (2018) 1028–1036.
[166] J. Liu, M. Yu, G. Zeng, J. Cao, Y. Wang, T. Ding, X. Yang, K. Sun, J. Parvizi, S. Tian, Dual antibacterial behavior of a curcumin–upconversion photodynamic nanosystem for efficient eradication of drug-resistant bacteria in a deep joint infection, J. Mater. Chem. B 6 (2018) 7854–7861.
[167] T. Zhang, D. Ying, M. Qi, X. Li, L. Fu, X. Sun, L. Wang, Y. Zhou, Anti-biofilm property of bioactive upconversion nanocomposites containing chlorin e6 against periodontal pathogens, Molecules 24 (2019) 2692.
[168] Y. Zhao, M. Hu, Y. Zhang, J. Liu, C. Liu, S.K. Choi, Z. Zhang, L. Song, Multifunctional therapeutic strategy of Ag-synergized dual-modality upconversion nanoparticles to achieve the rapid and sustained cidality of methicillin-resistant Staphylococcus aureus, Chem. Eng. J. 385 (2020) 123980.
[169] M. Qi, X. Li, X. Sun, C. Li, F.R. Tay, M.D. Weir, B. Dong, Y. Zhou, L. Wang, H.H. Xu, Novel nanotechnology and near-infrared photodynamic therapy to kill periodontitis-related biofilm pathogens and protect the periodontium, Dent. Mater. 35 (2019) 1665–1681.
[170] Z. Nie, X. Ke, D. Li, Y. Zhao, L. Zhu, R. Qiao, X.L. Zhang, NaYF4: Yb, Er, Nd@NaYF4: Nd upconversion nanocrystals capped with Mn: TiO2 for 808 nm NIR-triggered photocatalytic applications, J. Phys. Chem. C 123 (2019) 22959–22970.
[171] J. Xu, N. Liu, D. Wu, Z. Gao, Y.-Y. Song, P. Schmuki, Upconversion nanoparticle-assisted payload delivery from TiO2 under near-infrared light irradiation for bacterial inactivation, ACS Nano 14 (2020) 337–346.
[172] W. Fan, B. Yung, P. Huang, X. Chen, Nanotechnology for multimodal synergistic cancer therapy, Chem. Rev. 117 (2017) 13566–13638.
[173] B. Teng, C. Yu, X. Zhang, Q. Feng, L. Wen, C. Li, Z. Cheng, D. Jin, J. Lin, Upconversion nanoparticles loaded with eIF4E siRNA and platinum (IV) prodrug to sensitize platinum based chemotherapy for laryngeal cancer and bioimaging, J. Mater. Chem. B 5 (2017) 307–317.
[174] C. He, X. Duan, N. Guo, C. Chan, C. Poon, R.R. Weichselbaum, W. Lin, Core-shell nanoscale coordination polymers combine chemotherapy and photodynamic therapy to potentiate checkpoint blockade cancer immunotherapy, Nat. Commun. 7 (2016) 12499.
[175] K. Liu, X. Liu, Q. Zeng, Y. Zhang, L. Tu, T. Liu, X. Kong, Y. Wang, F. Cao, S.A. Lambrechts, M.C. Aalders, H. Zhang, Covalently assembled NIR nanoplatform for simultaneous fluorescence imaging and photodynamic therapy of cancer cells, ACS Nano 6 (2012) 4054–4062.
[176] S. Cui, D. Yin, Y. Chen, Y. Di, H. Chen, Y. Ma, S. Achilefu, Y. Gu, In vivo targeted deep-tissue photodynamic therapy based on near-infrared light triggered upconversion nanoconstruct, ACS Nano 7 (2013) 676–688.
[177] C. Li, D. Yang, P. Ma, Y. Chen, Y. Wu, Z. Hou, Y. Dai, J. Zhao, C. Sui, J. Lin, Multifunctional upconversion mesoporous silica nanostructures for dual modal imaging and in vivo drug delivery, Small 9 (2013) 4150–4159.
[178] Y. Liu, K. Ai, J. Liu, Q. Yuan, Y. He, L. Lu, A high-performance ytterbium-based nanoparticulate contrast agent for in vivo X-ray computed tomography imaging, Angew. Chem. Int. Ed. Eng. 51 (2012) 1437–1442.
[179] W. Jiang, C. Zhang, A. Ahmed, Y. Zhao, Y. Deng, Y. Ding, J. Cai, Y. Hu, H2 O2 -sensitive upconversion nanocluster bomb for tri-mode imaging-guided photodynamic therapy in deep tumor tissue, Adv. Healthc Mater. 8 (2019) e1900972.